Published in final edited form as:

Dev Cell. 2023 November 20; 58(22): 2614–2626.e7. doi:10.1016/j.devcel.2023.07.022.

Generation and application of endogenously floxed alleles for cell-specific knockout in zebrafish

Masahiro Shin[1], **Hui-Min Yin**[2,3], **Yu-Huan Shih**[1,7], **Takayuki Nozaki**[4], **Daneal Portman**[1,8], **Benjamin Toles**[1], **Amy Kolb**[1], **Kevin Luk**[1,9], **Sumio Isogai**[5], **Kinji Ishida**[4], **Tomohito Hanasaka**[4], **Michael J. Parsons**[6], **Scot A. Wolfe**[1], **Caroline E. Burns**[2,3], **C. Geoffrey Burns**[2,3], **Nathan D. Lawson**[1,10]

[1]Department of Molecular, Cell, and Cancer Biology, University of Massachusetts Chan Medical School, Worcester, MA 01605, USA

[2]Division of Basic and Translational Cardiovascular Research, Department of Cardiology, Boston Children's Hospital, Boston, MA 02115, USA

[3]Harvard Medical School, Boston, MA 02115, USA

[4]Technical Support Center for Life Science Research, Iwate Medical University, Shiwa, Iwate 028-3694, Japan

[5]Department of Medical Education, Iwate Medical University, Shiwa, Iwate 028-3694, Japan

[6]Department of Developmental and Cell Biology, School of Biological Sciences, University of California, Irvine, Irvine, CA 92697, USA

[7]Present address: Department of Pediatrics, University of Massachusetts Chan Medical School, Worcester, MA 01605, USA

[8]Present address: Westchester Medical Center, School of Medicine, New York Medical College, Valhalla, NY 10595, USA

[9]Present address: Excision Biotherapeutics, Inc., 499 Jackson Street, San Francisco, CA 94111, USA

[10]Lead Contact

SUMMARY

Correspondence: nathan.lawson@umassmed.edu (N. D. L.).

AUTHOR CONTRIBUTIONS

Conceptualization, M.S. and N.D.L.; Methodology, M.S., H-M.Y., Y-H.S., D.P.; Formal analysis, M.S., H-M.Y., N.D.L. Investigation, M.S., H-M.Y., Y-H.S., D.P., B.T., A.K.; Resources, T.N., K.L., S.I., K.I, T.H., S.A.W., M.J.P.; Writing – Original Draft, N.D.L.; Writing – Reviewing and Editing, M.S., H-M.Y., Y-H.S., S.A.W., C.E.B., C.G.B., N.D.L.; Visualization, N.D.L.; Supervision, C.E.B., C.G.B., N.D.L.; Funding acquisition, S.A.W., C.E.B., C.G.B., N.D.L.

DECLARATION OF INTERESTS

The authors declare no competing interests.

The zebrafish is amenable to variety of genetic approaches. However, lack of conditional deletion alleles limits stage- or cell-specific gene knockout. Here, we applied an existing protocol to establish a floxed allele for *gata2a*, but failed to do so due to off-target integration and incomplete knock-in. To address these problems, we applied simultaneous co-targeting with Cas12a to insert loxP sites in *cis*, together with transgenic counter-screening and comprehensive molecular analysis to identify off-target insertions and confirm targeted knock-ins. We subsequently used our approach to establish endogenously floxed alleles of *foxc1a, rasa1a, and ruvbl1,* each in a single generation. We demonstrate the utility of these alleles by verifying Cre-dependent deletion, which yielded expected phenotypes in each case. Finally, we used the floxed *gata2a* allele to demonstrate an endothelial autonomous requirement in lymphatic valve development. Together, our results provide a framework for routine generation and application of endogenously floxed alleles in zebrafish.

eTOC

The zebrafish is amenable to genetic approaches, but conditional gene knockout has been limited due the lack of floxed deletion alleles. Shin et al. describe reliable methods for generating, validating, and applying zebrafish bearing endogenously floxed alleles, providing a foundation for widespread application of conditional knockout approaches in zebrafish.

INTRODUCTION

The zebrafish has become a widely accepted model system for studying developmental biology based on several notable benefits of its life cycle. Zebrafish embryos are transparent and develop externally, allowing visualization of morphogenesis *in vivo*[1]. Embryogenesis is highly synchronous and rapid, with organ systems functioning by one to two days post fertilization (dpf)[2]. Coupled with these benefits is the genetic amenability of the zebrafish. Adults are easy to maintain and exhibit high fecundity, with a single pair often yielding hundreds of eggs on a given day. Zebrafish researchers leveraged these characteristics to perform large-scale forward genetic screens for a host of embryonic phenotypes[3–5]. Subsequent development of sequence-specific nucleases, such as those that target clustered regularly interspaced short palindromic repeats (CRISPR) in bacteria, has allowed introduction of targeted germline deletions in the zebrafish genome for reverse genetic approaches[6,7]. Thus, a combination of genetic accessibility and unique embryonic characteristics make the zebrafish an ideal model for interrogating gene function during development.

Nearly all zebrafish mutants perturb the function of a given gene from the earliest point at which it is expressed during development, making it a challenge to study direct roles in subsequent processes. While mosaic analysis through cell transplantation can address issues of cell autonomy in these mutants, ascribing primary functional effects at later stages remains challenging. Early efforts to address this issue relied on identification of temperature sensitive alleles, but these were limited[8]. More recently, conditional transgenic systems have been developed, but these require the use of dominant activating or inhibitory transgenes that may interfere with unrelated pathways[9]. Thus, a reliable and definitive

conditional genetics platform is lacking in zebrafish, limiting analysis at postembryonic and adult stages.

The mouse became an established genetic model through development of techniques for making germline deletions using embryonic stem cells[10–12]. Subsequently, mouse researchers leveraged this platform for conditional genetics using the Cre/lox system[13]. Cre is a bacteriophage recombinase that stimulates recombination between loxP sequences[14]. When loxP sites are arranged directly in *cis*, recombination deletes the intervening sequence. By modifying endogenous mouse loci to flank coding exons with loxP sites (referred to as "floxed"), together with transgenic expression of a cell-specific Cre, it is possible to achieve tissue-specific gene knockout[13]. Timing of the knockout can be controlled using Cre fused to a modified estrogen ligand binding domain that binds to tamoxifen (CreERT[15]). To date, there are over 3000 published floxed alleles for approximately 2300 mouse genes, along with more than 300 transgenic lines expressing CreERT, allowing comprehensive genetic analysis in any biological context.

DESIGN

In zebrafish, Cre/lox has been applied for lineage tracing and conditional transgene expression[9]. However, its application for conditional gene deletion in zebrafish has been limited by the difficulty in generating endogenously floxed alleles. Indeed, only two previous studies have successfully made such alleles in zebrafish. Burg et al. used single-stranded oligodeoxynucleotides (ssODNs) with short homology arm sequences and a loxP site as a template for homology-directed repair (HDR), together with generating a double-stranded break (DSB) the target site using Cas9 nuclease, to generate a floxed *tbx20* allele[16]. However, this approach inserted each loxP site sequentially, requiring two generations to establish a floxed allele. By contrast, Hoshijima et al. relied on plasmid template with 1kb homology arms to replace an endogenous exon of *potassium voltage-gated channel, subfamily H, member 6a* (*kcnh6a*) with a floxed version in a single generation[17]. In both cases, Cre-mediated excision of the floxed allele resulted in expected cardiac defects[16,17]. Here, we present our experience applying the Hoshijima et al. technique to generate a floxed *gata2a* allele, with a practical emphasis on pitfalls and points for improvement. We leveraged our experience to develop an improved protocol, which we applied to generate floxed alleles for *foxc1a*, *rasa1a*, and *ruvbl1*. Finally, we used the *gata2a* floxed allele with a tissue-specific inducible CreERT transgene to demonstrate an endothelial autonomous requirement during lymphatic valve development.

RESULTS

Generation of a *gata2a* conditional knock-in allele

To generate a floxed allele we applied the Hoshijima protocol[17] to target *gata2a*, which encodes a zinc finger transcription factor expressed in blood, endothelial cells, and neurons[18–20]. We constructed a targeting plasmid with homology arms 1 kb up- and downstream of exon 5, which was flanked by loxP sites (Figure 1A, B). Homology arms matched the haplotype sequence in adults used to produce embryos for injection, as recommended[17]. Immediately downstream of exon 5 we placed a *crystallin, alpha A* (*cryaa*)

promoter and enhanced green fluorescent (EGFP) cassette (Figure 1B; Supplementary File S1) to identify transgenic individuals by green lens fluorescence[21]. This cassette is flanked by FRT sites for removal if it interferes with normal gene function. The targeting cassette was flanked by I-SceI sites to release a linear HDR template[17]. Exon 5 deletion yields an in-frame exon junction that removes the C-terminal zinc finger (Supplementary Figure S1A, B), which is essential for DNA binding[22]. This allele is structurally the same as the widely used mouse Gata2^{tm1Sac} allele[23] (Supplementary Figure S1C).

To stimulate HDR, we used Cas9/sgRNA ribonucleoprotein complex (RNP) to introduce a DSB downstream of *gata2a* exon 5 (Figure 1A). In the targeting construct, we mutated the Cas9 spacer and split it from the PAM sequence with the 3' loxP site to prevent cleavage (Supplementary File 1). We co-injected 1-cell stage embryos with Cas9 RNP, targeting plasmid, and I-SceI. At 3 days post fertilization (dpf), PCR across the 3' homology arm junction revealed 6 out of 12 individual embryos exhibited a fragment of correct size and junction sequence in *cryaa:egfp*-positive embryos (Figure S2A–C). We repeated injections, grew *cryaa:egfp*-positive embryos to adulthood, and identified 12 founders out of 115 that transmitted *cryaa:egfp* to progeny embryos. Of these, only one (*gata2a^{um295}*) gave PCR-positive embryos with the primers above, suggesting that most founders carried off-target insertions.

Subsequent PCR analysis of *gata2a^{um295}* revealed that only the 3' loxP site and *cryaa:egfp* cassette inserted at the target (Supplementary Figure S2D–F), while Southern analysis revealed an off-target integration. Precise knock-in would yield a 7.7kb or 15kb fragment following digest of genomic DNA with ScaI or BstEII, respectively, and 4.7kb with a double digest followed by Southern hybridization using an Egfp probe (Figure 1C, D). However, additional fragments were also apparent indicating random insertion of the vector (Figure 1D). Unfortunately, this off-target integration co-segregated with *gata2a^{um295}* demonstrating linkage, although we did not detect Cre-mediated recombination between the off-target and single inserted loxP sites in *gata2a^{um295}* embryos (Supplementary Figure S3A, B). Therefore, we introduced a 5' loxP site upstream of the targeted exon 5 by first eliminating the off-target *cryaa:egfp* cassette (Supplementary Figure S3B, C; referred to as *gata2a^{um329}*, which retains some targeting construct sequence and a single loxP at the off-target site). We then injected homozygous *gata2a^{um329}* embryos with a Cas12a RNP targeted to a sequence upstream of exon 5 and a double-stranded (ds) ODN template with 30 bp flanking homology arms and a loxP site in direct orientation relative to the integrated 3' loxP site (Supplementary Figure S3C, D). We identified a founder with a precise 5' loxP integration (1 out of 15 fish screened; Supplementary Figure S3E) and the resulting floxed allele (*gata2a^{um345}*) is referred to as *gata2a^{fl}* (Figure 1C, E).

To test *gata2a^{fl}* functionality, we crossed *gata2a$^{+/fl}$* carriers to *gata2a$^{+/um27}$* adults, which bear a frameshift deletion upstream of the Gata2a zinc finger domains[24]. As expected, one-half of progeny embryos showed *cryaa:egfp* expression and retain exon 5 in the absence of Cre (Figure 2A, B; Supplementary Table S1). By contrast, *cre* mRNA injection caused loss of *cryaa:egfp* and exon 5 (Figure 2B, Supplementary Table S1). As expected[24], we also observed fully penetrant loss of swim bladder inflation in heterozygous *gata2a^{um27}* embryos with Cre-mediated exon 5 deletion (*gata2a$^{um27/\Delta}$*), while siblings were normal (Figure 2C,

Supplementary Table S1). Uninjected trans-heterozygous *gata2a*$^{um27/fl}$ larvae inflated their swim bladders at 5 dpf and appeared indistinguishable from *gata2a*$^{+/fl}$ siblings (Figure 2D). Consistently, *gata2a*$^{fl/fl}$ adults were viable and fertile. Uninjected *gata2a*$^{fl/fl}$ larvae from crosses between *gata2a*$^{fl/fl}$ and *gata2a*$^{+/fl}$ adults also expressed *cryaa:egfp* and displayed normal swim bladder inflation at 6 dpf (Figure 2E, Supplementary Table S2). By contrast, *gata2a*$^{fl/fl}$ larvae injected with a zebrafish codon-optimized *cre* mRNA (*zfcre*) at 1-cell stage showed loss of *cryaa:egfp* and no swim bladder inflation (Figure 2F, Supplementary Table S2).

We next assessed spinal neuron and circulatory defects in *gata2a*$^{fl/fl}$ embryos [18,19,24]. Uninjected *gata2a*$^{fl/fl}$ embryos express *urotensin related peptide 1* (*urp1*) in the ventral-most Kolmer-Agduhr (KA) neurons in the floor plate and *somatostatin 1, tandem duplicate 1* (*sst1.1*) in more dorsally-located KA neurons at 24 hours post fertilization (hpf; Figure 2G, H). By contrast, *urp1*-positive cells were absent in *gata2a*$^{fl/fl}$ embryos injected with *zfcre* mRNA, while *sst1.1*-expressing KA neurons were present (Figure 2I, J), similar to *gata2a*^{um27} mutant embryos[19]. *Gata2a*$^{+/fl}$ sibling embryos injected with *zfcre* mRNA exhibited a normal heartbeat and circulation throughout aortic arch blood vessels, with venous circulatory return from cranial vessels through the posterior cerebral vein and primary head sinus (Supplementary Movie S1). Trunk circulation through the dorsal aorta (DA) and posterior cardinal vein (PCV) was also normal (Supplementary Movie S1). In zfCre-injected *gata2a*$^{fl/fl}$ embryos, we observed a heartbeat and blood cell circulation through aortic arch blood vessels and cranial veins, albeit weaker than in *gata2a*$^{+/fl}$ siblings (Supplementary Movie S2). However, trunk circulation was absent (Supplementary Movie S2), similar to *gata2a*^{um27} mutants[24].

Analysis of *gata2a* transcript in *gata2a*$^{fl/fl}$ embryos by qRT-PCR using primers in exon 5 and 6 indicated expression in uninjected embryos, but not those injected with *zfcre* mRNA (Figure 2K). By contrast, *gata2a* transcript detected using 3' UTR primers was not reduced by exon 5 deletion, consistent with an in-frame exon 4/6 fusion (Figure 2L, Supplementary Figure S1B). Together, these observations indicate that *gata2a*^{fl} provides wild type *gata2a* function and Cre-dependent deletion of exon 5 in *gata2a*$^{fl/fl}$ phenocopies *gata2a*^{um27} mutants. Thus, *gata2a*^{fl} behaves as a conditional loss-of-function deletion allele.

Simultaneous dual CRISPR targeting can improve complete knock-in frequency.

In generating *gata2a*^{fl}, we failed to achieve complete knock-in, which we hypothesized was due to the location of the DSB. Our targeting strategy, which mirrored previous work[17], placed the Cas9 spacer at the 3' loxP insertion site, 340 downstream of the 5' loxP site (Figure 1A, B). This stretch of homology could allow HDR-mediated insertion of only the *cryaa* transgene and 3' loxP site. We reasoned that simultaneous DSBs at both loxP insertion sites would force HDR using the homology arms outside of the loxP sites, thereby improving complete knock-in. Alternatively, only targeting the site of 5' loxP insertion could better facilitate full knock-in since embryos screened for *cryaa:egfp* expression will likely also harbor the adjacent 3' loxP site. To test these possibilities, we identified CRISPR targets flanking *foxc1a*, which encodes a Forkhead transcription factor[25]. Since *foxc1a* is a single exon gene, we targeted immediately downstream of the promoter identified

by DANIO-CODE[26], and 150 bp downstream of the annotated 3' UTR (Figure 3A, B; Supplementary File S2). The loxP sites flank a 2.2 kb fragment comprising *foxc1a* coding and UTR sequences, and haplotype-matched homology arms extend 400 bp up- and 1kb downstream of these sites (Figure 3B; Supplementary File S2).

We used Cas12a as a nuclease since it can stimulate higher HDR rates than Cas9 and is amenable to targeting AT-rich non-coding sequence due to its 5'-TTTN PAM[27,28]. To compare effects of DSB location, we injected individual Cas12a RNPs targeting either loxP insertion site, or co-injected both RNPs, along with targeting plasmid and I-SceI. We assessed knock-in by PCR across 5' and 3' junctions in 10 individual *cryaa:venus*-positive embryos at 72 hpf in three replicate injections (Figure 3C; reverse primer for 5' product is anchored in the loxP site and does not detect endogenous *foxc1a*). Embryos injected with plasmid and I-SceI, but without RNP, do not exhibit knock-in but showed amplification with control primers to detect the endogenous locus (Figure 3D). Injections with only 3' RNP showed robust knock-in at the 3' junction, but not on the 5' side (Figure 3D, E). Conversely, 5' RNP induced robust 5' knock-in as well as 3' knock-in, though amplification appeared inconsistent and less robust on the 3' side (Figure 3D, E). Simultaneous injection of both RNPs further increased 3' knock-in while maintaining high rates of 5' knock-in (Figure 3D, E). Accordingly, the proportion of individuals exhibiting both 5' and 3' knock-in was significantly higher when comparing dual targeting to 3' RNP alone (Figure 3D, F). We also observed a benefit from targeting only the 5' insertion site, but this was less consistent (Figure 3F). Together, these results suggest that simultaneous dual CRISPR targeting is useful to stimulate complete knock-in of a floxed targeting cassette.

Transgenic counter-screening can identify germline carriers of off-target insertions.

Our *foxc1a* targeting construct included a cardiomyocyte-specific *myosin, light chain 7* (*myl7*) promoter:*mcherry* cassette outside of the homology arms to detect off-target insertions[17,29] (Figure 3B, Supplementary File S2). A plasmid bearing this cassette was previously described, but never applied[17]. To test the utility of this marker, we repeated dual RNP injections and separated 2 dpf embryos by *venus* and *mcherry* expression, followed by PCR across homology junctions (Figure 3C). One-third of injected embryos co-expressed *venus* and *mcherry* (19 out of 52) or only *venus* (19 out of 52). A smaller proportion exhibited only *mcherry* or no expression (7 out of 52 for each class). Surprisingly, only embryos co-expressing both transgenes consistently showed evidence of complete knock-in (Figure 4A), suggesting that *myl7:mcherry* does not distinguish on- and off-target integration at this stage.

We repeated injections, grew embryos that co-expressed *cryaa:venus* and *myl7:mcherry* to adulthood and identified founders. From 45 P0 fish, 7 gave progeny that were only double-positive for *cryaa:venus* and *myl7:mcherry*, with all but one being negative for 5' and 3' junction PCRs (for examples see embryo pools #4, 8, and 10 in Figure 4B, Supplementary Table S3). Two founders transmitted a mix of *cryaa:venus*;*myl7:mcherry* double-positive and *cryaa:venus* single-positive sibling embryos, one of which gave embryos with evidence of complete knock-in (Figure 4B, **founder 7;** Supplementary Table 3). We separately grew *cryaa:venus*-positive;*myl7:mcherry*-negative (*foxc1a*^{um383})

and *cryaa:venus;myl7:mcherry* double-positive (*foxc1a*^{um384}) embryos from founder 7. We then crossed individual *foxc1a*$^{+/um383}$ or *foxc1a*$^{+/um384}$ carriers and separated progeny based on transgene expression, followed by Southern blot analysis. In *cryaa:venus*-positive embryos from *foxc1a*^{um383} parents, we observed fragment sizes consistent with precise knock-in at the target, while genomic DNA from *cryaa:venus-negative* embryos did not hybridize to the Venus probe (Figure 4C, D; *foxc1a*^{um383} is hereafter referred to as *foxc1a*^{fl}). By contrast, we observed multiple fragments, none of the expected size, from double-positive *cryaa:venus;myl7:mcherry foxc1a*^{um384} embryos (Figure 4D), indicating multiple off-target insertions. These observations confirm that multiple germline insertions independently occurred in P0 founder 7 and demonstrate that transgenic counter-screening can distinguish F1 progeny bearing on- or off-target insertions.

We next crossed *foxc1a*^{fl} carriers to heterozygous *foxc1a*^{p162} adults, which bear a nonsense mutation in the Forkhead domain[30]. All resulting embryos appeared normal regardless of genotype indicating that the *cryaa:venus* cassette does not affect *foxc1a* function (Figure 4F). All sibling embryos injected with *cre* mRNA lack *cryaa:venus* expression, while *foxc1a*$^{p162/fl}$ embryos showed deletion of the floxed allele (*foxc1a*$^{p162/\Delta}$) and exhibited small eyes and cardiac edema (Figure 4E, G), as expected[31]. We also did not observe circulation in any *foxc1a*$^{p162/\Delta}$ embryos compared to relatively normal heterozygous and homozygous wild type siblings (Figure 4E), consistent with our previous findings[18]. Occasional circulatory defects in wild type embryos suggests mild toxicity from Cre itself in these experiments (Figure 4E). *Foxc1a*$^{fl/fl}$ homozygous adults were normal and fertile, while *foxc1a*$^{fl/fl}$ embryos injected with *zfcre* mRNA exhibited loss of aortic arch and trunk circulation (Supplementary Movies S3, S4). Accordingly, we observe loss of *foxc1a* expression following injection of *foxc1a*$^{fl/fl}$ larvae with *zfcre* mRNA and expression of *foxc1b* is unchanged (Figure 4H). Together, these observations demonstrate that *foxc1a*^{fl} behaves as a conditional loss-of-function allele following Cre-mediated deletion.

Generation of additional floxed alleles.

To further test our knock-in approach, we generated floxed alleles for *rasa1a* and *ruvbl1*, the latter of which was targeted by co-authors (H. M. Y., C. E. B., C. G. B.) in an independent lab. *Ruvbl1* (also known as *pontin*) encodes an ATPase required for chromatin modification and cilia assembly[32,33]. Since the conditional *Ruvbl1*^{tm1a} allele in mouse is a floxed exon 3, we generated a targeting construct to insert loxP sites flanking zebrafish *ruvbl1* exon 3 (Figure 5A, B). In this case, we used a single Cas12a RNP targeting the 5' loxP insertion site, based on our findings above (see Figure 3D–F). Targeting strategy and follow-up analyses were otherwise the same. From injected embryos, we screened eleven P0 adults via group in-crosses from which we observed embryos expressing *cryaa:venus* and *myl7:mcherry* or *cryaa:venus* only with evidence of both 5' and 3' insertions (Figure 5D). Subsequent individual outcrosses identified three founders that gave progeny expressing both *cryaa:venus* and *myl7:mcherry.* One P0 adult gave a mix of progeny expressing both transgenes or only *cryaa:venus*, the latter of which were positive for PCR across both 5' and 3' junctions and were grown to adulthood as *ruvbl1*^{chb10} (Figure 5C, D; hereafter referred to as *ruvbl1*^{fl}). We verified precise insertion and lack of off-target integration by Southern analysis of F2 *cryaa:venus*-positive progeny (Figure 5C, E). Homozygous *ruvbl1*$^{fl/fl}$ larvae

appeared normal (Figure 5F, G) and adults were viable and fertile. By contrast, *ruvbl1*$^{fl/fl}$ larvae injected with *zfcre* mRNA exhibit trunk curvature and cardiac edema (Figure 5F, G) as previously observed in *ruvbl1*^{hi1055b} mutant larvae[33], and loss of *ruvbl1* transcript containing exon 3 and an overall reduction of transcript (Figure 5H). These findings indicate that *ruvbl1*^{fl} functions as a conditional floxed allele.

RASA1 is a GTPase activating protein (GAP) that stimulates conversion of Ras-bound GTP to GDP, leading to Ras inactivation[34]. In humans, loss-of-function *RASA1* mutations lead to capillary and arteriovenous malformations[35], while mouse knockouts show embryonic vascular and lymphatic defects[36,37]. The zebrafish genome encodes two *RASA1* orthologs, *rasa1a* and *rasa1b*, for which mutants have not been described. Therefore, we first generated deletion alleles in each gene. Zebrafish larvae bearing a homozygous 5-bp deletion in the Rasa1a GAP domain leading to a frameshift (*rasa1a*^{um255}) show a low penetrance of ocular, gut and cardiac edema, and loss of circulation by 4 dpf. Phenotypic penetrance is significantly increased on a *rasa1b*^{um290} homozygous mutant background, with all double homozygous embryos displaying these defects (Figure S4A–C), while larvae only homozygous for *rasa1b*^{um290} are normal and viable. Based on these phenotypes, we inserted loxP sites flanking *rasa1a* exons 20 and 21, which encode part of the GAP domain and, when deleted, would lead to a frameshift similar to *rasa1a*^{um255} (Figures 6A, B, and S4A; Supplementary File 4). Following injection, we identified 4 out of 64 adults that transmitted *cryaa:Venus*, but not *myl7:mcherry*, one of which showed PCR amplification across both 5’ and 3’ junctions (Figure S4D, E; founder 5, referred to as *rasa1a*^{um414}). Southern analysis of *rasa1a*^{um414} progeny supported knock-in at the target, although a MscI fragment appeared larger than expected (Figure 6D). PCR across the 5’ junction in *rasa1a*^{um414} embryos using conditions that favored long amplification yielded a 4.5 kb fragment that included the polyadenylation signal from the *myl7:mcherry* cassette, ampicillin resistance and lacZ genes, and intact I-SceI sites (Figure S4F, Supplementary File 5). This suggests that *rasa1a*^{um414} arose from HDR mediated repair on the 3’ end and non-homologous end joining-mediated insertion of the 5’ homology arm and vector sequence. The initial positive 5’ PCR (see Figure S4D) likely resulted from spurious internal priming between tandem duplicate 5’ homology arm sequences, similar to previous observations[38,39]. Despite this insertion, *rasa1a*^{fl}*;rasa1b*^{um290} double homozygous individuals exhibited normal embryonic development (Figure 6E, G) and were viable and fertile as adults, while exhibiting fully penetrant edema and loss of circulation following injection of mRNA encoding zfCre at 1-cell stage (Figure 6E–G). Quantitative RT-PCR showed complete Cre-dependent loss of *rasa1a* mRNA containing exon 21, with reduction of total *rasa1a*, but not *rasa1b* transcript in *rasa1a*^{fl} homozygous mutants (Figure 6H). These observations demonstrate that the exogenous vector sequence inserted upstream of exon 20 does not affect *rasa1a* function and that *rasa1a*^{fl} acts as conditional deletion allele.

Endothelial cell-specific *gata2a* knockout causes defective lymphatic valve development

To demonstrate the application of a floxed allele for cell and stage-specific knockout in zebrafish, we used *gata2a*^{fl} to determine the endothelial autonomous requirement for *gata2a*. For this purpose, we developed a transgenic line where CreERT^2 was driven by *gata2aECE*, an intronic *gata2a* enhancer element that expresses in endothelial cells[18]

(Figure 7A). In this case, we incorporated *cryaa:mcherry* as a marker to identify transgenic carriers. We identified a founder from which progeny embryos displayed endothelial-specific recombination (*Tg(gata2aECE:CreERT2;cryaa:mcherry)*^{um337}; referred to as *gata2aECE:iCre*) and bred this line out to obtain a single copy insertion (Figure 7B). To confirm inducible endothelial-specific Cre activity, we crossed *gata2aECE:iCre* to fish bearing *Tg(ubb:loxP-cerulean-loxP;h2b-cherry)*^{ih63}, in which cells expressing Cre will switch to expressing a nuclear-localized form of mCherry[40] (referred to as *ubb:SwitchRed*). *Gata2aECE:iCre;ubb:SwitchRed* embryos show endothelial-specific H2B-mCherry expression at 6 dpf when exposed to 5 μM 4-hydroxytamoxifen (4OHT) from 1 to 3 dpf (Figure 7C, D). We observed H2B-mCherry in endothelial cells lining the facial lymphatic vessels, as well as those in aortic arch and brain blood vessels (Figure 7C). In trunk vessels, H2B-mCherry was restricted to endothelial cells within the posterior cardinal vein and the thoracic duct, with mosaic expression in intersegmental vessels and very few cells apparent in the dorsal aorta (Figure 7D).

We incrossed *gata2a*$^{+/fl}$*;gata2aECE:iCre* adults and treated resulting progeny with DMSO or 4OHT from 1 to 3 dpf. Homozygous *gata2a*$^{fl/fl}$ larvae without iCre, identified by *cryaa:egfp* but not *cryaa:mcherry* and confirmed with genotyping, exhibited inflated swim bladders and normal circulation (Figure 7E, G). By contrast, 4OHT-treated *gata2a*$^{fl/fl}$;*gata2aECE:iCre* larvae (referred to hereafter as *gata2a*$^{i\Delta EC}$) displayed edema around the eyes and gut at a penetrance similar to that of whole body *gata2a* knockout larvae[18] (Figure 7F, H). In these experiments, we initially identified *gata2a*$^{i\Delta EC}$ larvae by lens expression of mCherry and Egfp, followed by genotyping for *gata2a*$^{fl/fl}$. In contrast to *cre* mRNA injection (see Figure 2F), *gata2a*$^{i\Delta EC}$ larvae retain *cryaa:egfp* due to the specificity of CreERT^2 expression (Figure 7F). Despite lymphedema, *gata2a*$^{i\Delta EC}$ larvae were otherwise normal, with inflated swim bladders and active trunk circulation (Figure 7E, F), unlike *gata2a*^{um27} mutants[18]. Furthermore, *gata2a*$^{i\Delta EC}$ embryos treated from 6 hpf to 24 hpf with 4OHT exhibited normal *urp1* expression in ventral KA neurons (Figure 7I, J), unlike *gata2a*$^{fl/fl}$ embryos injected with *zfcre* mRNA (Figure 2I). Quantification of *gata2a* transcript in H2B-mcherry-positive cells isolated by fluorescence activated cell sorting (FACS) from *gata2a*$^{i\Delta EC}$ larvae bearing *ubb:SwitchRed* (i.e. cells having exhibited Cre-mediated recombination) showed significant reduction in transcript containing exon 5, but not the 3' UTR, compared to wild type or *gata2a*$^{+/i\Delta EC}$ larvae (Figure 7K). In contrast to *gata2a*$^{fl/fl}$ embryos injected with *zfcre* mRNA, wild type transcript was still detectable in *gata2a*$^{i\Delta EC}$ larvae at low levels suggesting that recombination was robust, but incomplete when using *gata2aECE:iCre* (compare with Figure 2K, L).

Edema in *gata2a*^{um27} mutant embryos coincides with defects in lymphatic valve formation[18]. Therefore, we performed electron microscopy to investigate lymphatic valve morphology. In wild type larvae at 7 dpf, we observed flattened bicuspid valve leaflets separating the facial collecting lymphatic vessel (FCLV) and lateral facial lymphatic vessel (LFL), as previously described[18] (Figure 7L). By contrast, lymphatic valve leaflets appeared disorganized in *gata2a*$^{i\Delta EC}$ larvae that had been treated with 4OHT from 1 to 3 dpf. We observed multiple leaflets spanning the lumen between the FCLV and LFL in a disorganized manner (Figure 7M), similar to what we have previously observed in *gata2a*^{um27} mutant larvae[18].

DISCUSSION

In this work we describe our efforts to generate and apply floxed deletion alleles in zebrafish. Our initial application of a previous knock-in protocol for this purpose led us to identify several important caveats and points for improvement. We subsequently leveraged our experience to develop a robust pipeline that we applied to establish floxed alleles for three loci, each in a single generation. Importantly, one of these alleles was generated in an independent lab, underscoring the utility of our approach within the zebrafish community. Together, our efforts here provide a blueprint for more widespread generation and application of floxed alleles in zebrafish.

The starting point for generating a floxed allele is target exon considerations. For *gata2a* and *ruvbl1* we implemented targeting strategies based on mouse alleles. Zebrafish and mouse genes often have conserved organization and functional domains making this a reliable approach. Indeed, both *gata2a*^{fl} and *ruvbl1*^{fl} behave as expected for conditional deletion alleles. Alternatively, genotype and phenotype characteristics of existing zebrafish mutants should be considered, as we did for *rasa1a*. Once a target is identified, sequencing the region in wild type adults is essential to match homologous arm sequences with the haplotype of injected embryos[17]. This also ensures proper design of PCR primers and CRISPR targets. While we did not directly test the effects of using non-homologous sequence, there is considerable variability between and within wild type zebrafish strains[41,42] and minor sequence variants in mouse significantly reduce knock-in rates[43].

An important targeting consideration in generating floxed alleles is location of the CRISPR-induced DSB relative to loxP sites and homology arms. At the *gata2a* locus a DSB at the 3’ loxP insertion site only achieved partial knock-in, likely due to sufficient homologous sequence for HDR downstream of the 5’ loxP site within the targeting construct. Moving the DSB to the 5’ loxP slightly improved knock-in in P0 individuals at the *foxc1a* locus and we used this approach to successfully establish the *ruvbl1*^{fl} allele. Simultaneous dual CRISPR targeting was even more robust for *foxc1a*, where there was a much larger span between the loxP sites. Therefore, for shorter targets (e.g. a single exon less than 500 bp), we suggest targeting a DSB to the loxP insertion site (the 5’ loxP target in our designs) opposite of that adjacent to the *cryaa* marker. While it is still likely that partial knock-in events will occur when targeting only the 5’ site, screening for *cryaa:venus* expression should reduce the occurrence of these types of insertions. To introduce DSBs, we employed Cas12a instead of Cas9. Unlike Cas9, which yields blunt ends, Cas12a leaves overhangs, while its PAM sequence lies opposite its cleavage site and the spacer can be up to 24 nucleotides[44]. Thus, initial indels created by Cas12a-stimulated cleavage can often be re-targeted. Together, these characteristics likely contribute to the ability of Cas12a to stimulate higher HDR rates than Cas9 in both zebrafish and mammalian cells[27,28]. The TTTN PAM used by Cas12a also favors its application for targeting AT-rich non-coding sequences used for intronic loxP insertion sites in floxed alleles.

An issue with targeted knock-in in multiple models is that non-homologous endjoining is favored over HDR as a repair event, leading to robust random insertion of the targeting construct. Indeed, the first protocols for generating targeted knockouts in mouse ES cells

incorporated a counter selection approach to reduce off-target insertions[12]. Accordingly, random integration occurred in most P0 founders across all targeted loci in our study. To reliably identify these events and confirm targeted knock-in, we successfully employed a combination of transgenic screening and molecular approaches. Transgenic counter-screening allowed us to clearly distinguish F1 individuals with on- and off-target insertions. However, this approach was not effective in injected embryos, where predominance of random insertions expressing both *cryaa:venus* and *myl7:mcherry* over rare HDR-mediated events likely masks identification of the latter. We also demonstrate that molecular validation by Southern analysis is essential to assess confirm precise integration and further rule out random integration. While considered a dated technical approach, it provides the simplest and most definitive means to identify off-target insertions in an unbiased manner. Our results with *rasa1a*^{fl} further underscore the importance for Southern analysis as a final molecular validation step since initial PCR screening of F1 progeny proved to be spurious. Several previous studies have demonstrated similar cases where false-positive PCR can confound identification of bona fide knock-in founders[38,39], making orthogonal validation approaches essential. Indeed, given the spectrum of different insertion events that we observed in our work, we strongly recommend a combination of PCR analysis coupled with transgenic counter screening and subsequent validation by Southern analysis to definitively validate endogenously floxed alleles.

Our results using *gata2a*$^{fl/fl}$ demonstrates the utility of floxed alleles for genetic analysis at zebrafish larval stages. We previously relied on the *gata2a*^{um27} allele, which causes numerous embryonic defects that can confound analysis at larval stages[18,24], a common issue with most zebrafish mutants. Notably, *gata2a*^{um27} mutant embryos have circulatory defects that could indirectly affect lymphatic valve development, which is sensitive to mechanosensory input in other models[45]. By contrast, *gata2a*$^{i\Delta EC}$ larvae displayed normal circulation and neuronal specification, yet defects in lymphatic valve function and morphogenesis with a severity and penetrance similar to *gata2a*^{um27} mutants[18]. This observation is consistent with the known endothelial autonomous role for mouse *Gata2* in lymphatic valve formation[46]. Of note, normal circulatory function in *gata2a*$^{i\Delta EC}$ embryos was somewhat surprising given the severity of circulation defects in *gata2a*^{um27} embryos and endothelial expression of *gata2a* in embryos[18,24]. It is possible that *gata2a* acts at a stage prior to the 4OHT treatment used in our experiments. Alternatively, *gata2a* acts in endothelial subtypes not targeted by *gata2aECE:iCre*. For example, *gata2aECE:iCre* did not induce recombination in arterial endothelial cells, raising the possibility that only this cell type in the trunk blood vessels is affected by loss of *gata2a*. The possibility also remains that circulatory defects in *gata2a*^{um27} embryos are not endothelial autonomous. In any case, the availability of the *gata2a*^{fl} allele, together with other Cre lines, now allows us to better investigate the cellular nature of the early circulatory defects.

The development of efficient CRISPR nucleases now enables zebrafish researchers to engineer knock-in alleles. Initial efforts in this regard introduced short epitope tags or reporter transgenes using a single DSB to insert exogenous sequence[6,17,47]. More recent studies have used a single DSB with a plasmid targeting vector to insert a conditional splice trap cassette into an intron via HDR[48–50]. These alleles also incorporate reporter transgenes to observe endogenous expression and to assess Cre-mediated recombination. However,

splice traps may not always lead to loss-of-function and reliable reporter expression is limited to strongly expressed genes. Moreover, splice traps will not work for small genes comprising only one or two exons. In general, a floxed deletion allele is more likely to be definitively loss-of-function. Although these alleles can be more challenging to make, the improvements we have identified should aid researchers in this regard. The mouse community currently benefits from thousands of floxed alleles and hundreds of Cre lines allowing genetic analysis in any setting. These tools have enabled the mouse to become the preeminent genetic model for studying vertebrate development. The zebrafish is currently constrained by the lack of such tools. We hope that our efforts here can serve as an initial framework to establish more floxed lines that allow conditional gene manipulation in zebrafish.

Limitations of the study

Our protocol for targeted gene replacement in a single generation remains labor- and time-intensive and rates of precise knock-in can still be variable. Our approach also requires techniques that are no longer commonplace in most labs and considered dated (e.g. Southern analysis), but nonetheless proved to be essential. Further advances can likely be made to improve knock-in rates, including optimization of template topology[51] and other parameters that govern HDR. Despite these limitations, our work underscores that it is feasible to routinely generate floxed zebrafish lines and that careful validation is essential to successful implementation of our approach.

STAR METHODS

RESOURCE AVAILABILITY

Lead Contact—Information and requests for resources and reagents should be directed to and will be fulfilled by the lead contact, Nathan Lawson (nathan.lawson@umassmed.edu)

Materials availability—Plasmids generated in this study are available by request from the lead contact. Transgenic and knock-in zebrafish lines are available by request from the lead contact.

Data and code availability—All original data and images are available from the Lead Contact upon request. This paper does not report original code.

Any additional information required to reanalyze the data reported in this work paper is available from the Lead Contact upon request.

EXPERIMENTAL MODEL AND STUDY PARTICIPANT DETAILS

Animals—All zebrafish used in this study were handled according to approved University of Massachusetts Chan Medical School and Boston Children's Hospital Institutional Animal Care and Use Committee protocols. Establishment and characterization of *gata2a*^{um27}, *foxc1a*^{p162}, and *Tg(ubi:CtoH2b-cherry)*^{jh63} lines has been described elsewhere[24,30,40]. Generation of all other alleles is described below. All adult zebrafish were maintained at 28°C in a recirculating system. All analysis was performed on embryos or larvae at indicated

stages. All stages under investigation in this study are prior to specification of sex in zebrafish, therefore this was not considered as a variable.

METHOD DETAILS

Target locus sequencing—We sequenced target loci in genomic DNA isolated from finclips from 12 individual TL wild type fish (6 males and 6 female). For *gata2a*, we amplified by PCR using superPfx (Cowin Biotech) using primers: 5'-GGGGAATTGCGCTGTACGCCTATAAA-3' and 5'-AATATGGACCTTTGAGGTACCACCCC-3' to obtain genomic sequence flanking exon 5 (GRCz11, chr11:3,849,652–3,852,157). For *foxc1a*, we used primers: 5'-CTTAACCTCGCTGTATGGCTGTAG-3' and 5'-CCCACAAGGCAGTGGCTAGCAGAACTCATG-3' to amplify a spanning genomic sequence (chr2:686,529–689,296) of upstream including 5' homologous arm, promoter, coding exon and 3'UTR, and 5'- CGGGAATAACAGCTGTCAAATGTC-3' and 5'-AACCGCTGTAATCACTACCAACCGCTCATG-3' to amplify 3' homologous sequence (chr2:685,341–687,455). Amplicons were cloned into pBluescript linearized with SmaI. For *rasa1a*, we used 5'-GCGTGTACGTCCATCTTGCGAATGTAC-3' and 5'-CAACTGCCTCATATCAACTATTCAGGCTG-3' to obtain genomic sequence flanking exon20 and exon21 (chr5:47,953,001–47,954,255) subcloned into pCR Blunt II TOPO vector using Zero Blunt TOPO PCR cloning kit (ThermoFisher). We sequenced individual clones from each ligation and aligned them to reference genomic sequence (GRCz11). For embryo generation for injection, we used a male and a female bearing the same haplotype for each locus that also matched the homology arms in the respective targeting construct (see Supplementary Files 1–4).

Plasmid construction—For generation of a *gata2a* targeting vector, 5' and 3' homologous arms corresponding to GRCz11 chr11:3,851,035–3,852,157 and chr11:3,849,652–3,850,708, respectively, were PCR-amplified from sequence validated pBluescript clones described above. After digestion of pBS-ISceI using ClaI and SacII in MCSs, these PCR products were combined with a gBlock DNA fragment (IDT) containing *gata2a* exon 5 genomic sequence (chr11:3,850,717–3,851,034), a 5' loxP sequence, FRT-flanked *cryaa:egfp*, and a 3' loxP site in a HiFi Assembly reaction (NEB) with pBS-ISceI to give pBSIce-gata2aKI (Supplementary File 1).To construct a *foxc1a* targeting vector, 5' loxP sequence and point mutations (5'-TTTC-3' to 5'-CCCT-3') on the Cas12a RNP1 PAM sequence were added in the upstream of the promoter sequence (chr2:689,007) in pBluescript vector described above. DNA fragments of modified *foxc1a* locus with 5' homologous arm (chr2:689,008–689,404) and loxP, and 3' homologous arm (chr2:685,632–686,723) were separately PCR-amplified from the vectors. After digestion of pKHR8 (Addgene#74625; Hoshijima et al. 2016) using BamHI and SalI in MCSs, the DNA fragments were assembled using NEbuilder HiFi DNA assembly kit to give pKHR8-foxc1aKI (Supplementary File 2). To construct a *rasa1a* targeting vector, gBlock encoding *rasa1a* genomic sequence (chr5:47,953,030–47,953,972) encompassing the 5' homology arm (chr5:47,953,030–47,953,311), exons 20 and 21 with a BamHI-5' loxP-NotI sequence to disrupt the Cas12a RNP1 target was synthesized (IDT) while 3' homologous arm (chr5:47,953,973–47,954,995) was PCR-amplified from sequence-validated plasmid

described above. After digestion of pKHR8 using BamHI and SalI, the gBlock and PCR amplicons were assembled using NEbuilder HiFi DNA assembly kit to give pKHR8-rasa1aKI (Supplementary File 4). To construct a *ruvbl1* targeting vector, the 5' homology arm (chr6:40,832,688–40,841,106) was PCR-amplified with 5'-GCGGGTCTCTTGTGTTTGATTTTAACG-3' and 5'- CCTTACCTTGCCTGTTCCAG -3', the 5'-loxp and mutated CRISPR target site were introduced by NEbuilder HiFi DNA assembly kit with 5'-TATAACTTCGTATAGCATACATTATACGAAGTTATAGTTTCAGAGCTGTTGTTTAAGATAGTATGTATAGTCTGCCCATTTGATTTCTATCCA-3' and 5'-GACTGGTTTTATTTACACTGCACTCTATATTTATAATGGTCAATATAATATAACTTCGTATAGCATACATTATACGAAGTTATAG-3'. The 3' homology arm (chr6:40,834,179–40,845,039) was PCR-amplified with 5'- TCAACTTGCCGTGGTAAACAAATATGGG-3' and 5'- TTGATACGCAGACCTGTTCG-3'. All the fragments were sequentially assembled into pKHR8 vector by NEbuilder HiFi DNA assembly kit. A Cre Gateway middle entry clone was generated by PCR using 5'-GGGGACAAGTTTGTACAAAAAAGCAGGCTTGACCaTGCCCAAGAAGAAGAGG-3' and 5'-GGGGACCACTTTGTACAAGAAAGCTGGGTAatcgccatcttccagcaggcg-3', followed by BP cloning into pDONR221 (ThermoFisher), to give pME-CreNS. pCS-CreNS was constructed via a multisite LR reaction using pCSDest2, pME-CreNS and p3E-MCS1 [52,53]. Alternatively, we used a Cre with zebrafish optimized codon usage (zfCre). For this purpose, we first constructed pME-zfCreERT^2 by HiFi assembly using two gBlock DNA fragments (IDT) and pME-MCS1 vector [54] linearized by inverse PCR using primers (5'-GTGAGTCGTATTACATGGTCATAGCTG -3' and 5'-GGCCGTCGTTTTACAACGTCGTGACTG -3'). To generate pME-zfCre, pME-zfCreERT^2 was digested using XhoI to remove zfERT^2 and self-ligated. We constructed pCS-zfCre using pCSDest2, pmE-zfCre and p3E-MCS1 in a multisite reaction using LR Clonase II (Thermofisher). For transgenic expression of CreERT^2, we first modified the Tol1 backbone vector, pToneDest (Addgene#67969)[55], by adding a *cryaa:mcherry* cassette to give pToneDestCryR. We then performed a multisite reaction using LR Clonase II with pToneDestCryR, p5E-6xgata2aECEbas [18], pENTR/D-CreERT2 (Addgene#27231)[56], and p3E-MCS1 to give pTol1-gata2aECE:CreERT^2;cryaa:mcherry.

***In vitro* transcription—**To synthesize *cre* and *zfcre* mRNA, we performed *in vitro* transcription using a mMESSAGEmMACHINE SP6 kit (ThermoFisher) with respective pCS vectors linearized with NotI (NEB). To synthesize Cas9 sgRNA, we annealed the following oligonucleotides: 5'-tagGAGAGGGACGAGCGAGGCC, 5'- aaaCGGCCTCGCTCGTCCCTCT and cloned them into pDR274 digested with BsaI to give pDR274-gata2a_3pex5sgRNA1. The resulting plasmids was linearized with HindIII (NEB) and used to synthesize sgRNA using the T7 MEGAscript kit (ThermoFisher). Preparation of DNA templates and generation of crRNAs targeting *gata2a* (5' site for loxP insertion RNP spacer; 5'-ACATGACCATGGGGTTGTTCCTT-3'), *foxc1a* (5'RNP target: 5'-CGATGCGCGCTCCGAGAGAAAGAG-3'; 3'RNP spacer: 5'CTGCGGCACACTTGAACGATCGTC-3'), *rasa1a* (5' RNP spacer: 5'- TGAAAATGTATTATTAATGCCTTG -3'; 3' RNP spacer: 5'-GTAAAATGAAAATAACATATTATA-3'), and ruvbl1 (RNP spacer: 5'-

ATGTCCATTTTAATTATACAGTG-3') with a full length direct-repeat for *Lachnospiraceae bacterium* Cas12a were performed as described previously [57], using bottom strand oligos (5'-TGACCATGGGGTTGTTCCTTATA ATCTACACTTAGTAG-3', 5'-CTCTTTCTCTCGGAGCGCGCATCG ATCTACACTTAGTAG-3' and 5'- GACGATCGTTCAAGTGTGCCGCAG ATCTACACTTAGTAG-3', 5'CAAGGCATTAATAATACATTTTCA ATCTACACTTAGTAG-3' and 5'-TATAATATGTTATTTTCATTTTAC ATCTACACTTAGTAG-3', respectively). Tol1 transposase mRNA was synthesized from linearized pToneTP as described elsewhere [55].

SpCas9 and LbCas12a Protein purification—3xNLS-SpCas9 protein expression and purification was performed as previously described[58]. LbCas12a-2xNLS protein expression and purification was performed as previously described[57].

Line generation—For targeting *gata2a*, 50pg of pBSIce-gata2aKI, 60pg of sgRNA, 0.8pg of 3xNLS-SpCas9 protein and 1mU of I-SceI (NEB) was injected per embryo at early 1-cell stage. At 2 dpf, embryos were separated based on expression of EGFP in the lens. Genomic DNA from individual embryos was purified by adding 50μL of 0.05M NaOH, incubating at 98°C for 10 minute, and then adding 10μL of 0.5M Tris pH7.5 (HCl). Precise knock-in of 3' homologous arm was evaluated by PCR using KAPA2G Fast HotStart ReadyMix (KAPA Biosystems) with a primer set (5'-CCACTAGTTCTAGAGCGGC-3' and 5'-GAACTGTTGGCTACTAACACTAATACTG-3') across the junction with endogenous sequence using genomic DNAs of individual embryos as templates. Subsequently, injected embryos with EGFP lens expression were grown to adulthood. Founders were screened by individual outcross with wild type adults followed by screening for lens expression of EGFP in progeny. The same primer set as above was used for PCR screening of genomic DNA from pooled embryos with lens EGFP expression. To delete the off-target loxP-flanked exon5 sequence, we injected 10 pg of *cre* mRNA into embryos from an incross of *gata2a*$^{um295/um295}$ parents and grew these to adulthood to give rise to *gata2a*^{um329}. To insert a loxP site 5' of the targeted *gata2a* exon 5 in *gata2a*^{um329} fish, we designed oligodeoxynucleotides (ODN) to include loxP sequence flanked by XhoI and EcoRI restriction sites and 30bp of homology (IDT). ODNs were annealed in 50mM NaCl solution to generate double stranded ODN template (dsODN) by incubating at 98^{o}C for 10 minutes followed by 95°C, 90°C, 85°C, 80°C, 75°C, 70°C, 65°C and 63°C each for 20 seconds before 62°C. We co-injected 45pg of dsODN and 57 fmol of LbCas12a-2xNLS RNP (see above) per embryo at early 1-cell stage. Embryos were derived from an incross of homozygous *gata2a*$^{um329/um329}$ adults. After injection, integration was evaluated by PCR using 5 PRIME HotMasterTaq DNA polymerase (Quantabio; primers : 5'-TTAGAAGAACCGGTCTTCAGTATG-3' and 5'CTGTAGGCAAGAAAGCAGAGTATTGTCA-3') on genomic DNA of pooled or individual embryos followed by digest with XhoI (NEB). Following validation of knock-in, injections were repeated and embryos grown to adulthood. Founders were identified using the same PCR primers and XhoI digestion as above. For generation of *foxc1a*^{um383}, 40 pg of pKHR8-foxc1aKI, 9.5 fmol of Cas12a 5' RNP, 9.5 fmol of Cas12a 3' RNP and 1mU I-SceI were co-injected into wild type TL embryos at early 1-cell stage. Injected embryos were sorted at 2 dpf for expression of Venus

in the lens and/or mCherry in the heart. Integration was evaluated by PCR using KAPA2G Fast HotStart ReadyMix on genomic DNA from individual embryos with primer sets that span 5' and 3' junctions between homology arms and endogenous sequence (5' junction primers; 5'- CAGATTTTACCTCTGGGTATTATACGA-3' and 5'- TACTGGCCACCTCTTATAACTTC-3', 3' junction primers; 5'- GATGAAGCTACATGGCTGTAGAACGTCAG-3' and 5'- AACCGCTGTAATCACTACCAACCGCTCATG-3'). After initial analysis, injections were repeated and only embryos expressing both Venus and mCherry were grown to adulthood. Founders were screened by individual outcross to wild type followed by screening for Venus and mCherry expression at 3 dpf. Embryos were separated based on Venus and mCherry expression, then pooled and used to isolate genomic DNA. We performed PCR across 5' and 3' junction sequences as above. For generation of *rasa1a*^{um414}, 18pg of pKHR8-rasa1aKI, 1.25 fmol of Cas12a RNP1, 1.25 fmol of Cas12a RNP2 and 1mU I-SceI were co-injected into wild type TL embryos at 1-cell stage. Similarly, somatic integration of embryos at 2 dpf after sorting for expression of GFP in lens and mCherry in heart was evaluated by PCR on individual genomic DNAs using 5' and 3' junction primer sets (5' junction primers; 5'-GCGTGTACGTCCATCTTGCGAATGTAC-3'and 5'- TACATTTTCAGCGGCCGCATAACTTC-3', 3' junction primers; 5'- GATGAAGCTACATGGCTGTAGAACGTCAG-3'and 5'- CAACTGCCTCATATCAACTATTCAGGCTG-3') (Figure S7C). For founder screening, embryos were sorted for Venus and mCherry expression at 3 dpf and pooled to isolate genomic DNA for PCR evaluation using 5' and 3' junction primer sets described above. After isolating *rasa1a*^{um414} allele and western blot assay to confirm single insertion, we noticed a nonspecific insertion of targeting vector sequence upstream of 5' homologues arm and PCR-amplified the insertion using flanking primers (5'-CAGATCAGACAGAGATCTACATGCATC-3 and 5'-TACATTTTCAGCGGCCGCATAACTTC-3') followed by whole PCR product sequence (Plasmidsaurus). For generation of *ruvbl1*^{fl}, 50 pg of pKHR8-ruvbl1, 24 fmol of Cas12a RNP, and 1mU I-SceI were co-injected into wild type TL embryos at early 1-cell stage. The integration was evaluated by PCR with primer sets that span 5' and 3' junctions between homology arms and endogenous sequence. (5' junction primer: 5'-CCCACAGCGTAGATCCTTGT-3' and 5'-GGGAGGATTGGGAAGACAAT-3', 3' junction primer: 5'-GCACTGAATGGCTCAGACAA-3' and 5'-TGCCTGCACTTCCTTACCTT-3').

To generate an endothelial-specific inducible Cre line, we co-injected 25 pg of pTol1-gata2aECE:CreERT^2 and 50 pg of Tol1 transposase mRNA into wild type 1-cell stage embryos. Only embryos expressing mCherry in the lens were grown to adulthood. Founders were identified by individual outcross and screening of progeny for mCherry lens expression at 3 dpf. Founders were subsequently validated by crossing to an adult bearing *Tg(ubi:CtoH2b-cherry)*^{jh63} followed by tamoxifen treatment. A founder was identified that gave robust endothelial recombination and designated as *Tg(gata2aECE:CreERT*^{2}*;cryaa:mcherry)*^{um337}. Following successive outcrosses with wild type, *Tg(gata2aECE:CreERT*^{2}*;cryaa:mcherry)*^{um337} a single copy insertion of the transgene was confirmed by Southern analysis (see below).

mRNA Injections—To delete loxP-flanked sequences we injected 10 to 25 pg of *cre* mRNA, or 6.25pg of *zfcre* mRNA into incrosses of fish that were heterozygous or homozygous for *gata2a*^{um345} or *foxc1a*^{um383} as indicated in the text.

Tamoxifen administration—A 10 mM 4-hydroxytamoxifen (4OHT; MilliporeSigma) stock solution was made by dissolving in DMSO, aliquoted, and stored at −80°C. For treatment, embryos were treated for the indicated timepoints by dissolving 10 mM stock to a final of 5 or 10 μM in standard egg water. In cases where larvae were to be subjected to confocal imaging, embryos were also treated with 0.003% phenylthiourea (PTU). Embryos were placed in egg water with fresh 4OHT every 24 hours. After the indicated treatment period, embryos were washed several times and maintained in PTU until 6dpf for imaging. For scanning electron microscopy (SEM), embryos were treated with tamoxifen at 5 μM between 1 dpf and 3 dpf grown until 7 dpf. Larvae were then analyzed by SEM and genotyped as described previously[18].

Fluorescent-activating cell sort (FACS)—FACS was performed at room temperature using cells dissociated from embryos carrying the *gata2a*$^{um345/um345}$, *gata2a*$^{+/um345}$ or *gata2a*$^{+/+}$, carrying transgene of the *Tg(gata2aECE:CreERT*^{2}*;cryaa:mcherry)*^{um337} and *Tg(ubi:CtoH2b-cherry)*^{jh63} at 5 dpf or 6 dpf with 4OHT administration between 6 hpf and 4 dpf under PTU treatment. Briefly, embryos (n=300 to 500) in 1x TrypLE (ThermoFIsher) at 28.5°C were minced with razor blade, dissociated within 15 minutes using P1000 pipetman (Gilson), and strained using 40μm pore-sized cell strainer (Falcon). Trypsin was inactivated by adding fetal bovine serum and cells rinsed with Leibovitz's L-15 media without phenol red (ThermoFisher). Cells were spun down at 300g for 5 minutes at room temperature and resuspended with collection solution (L-15 media/10% embryo extract) for FACS. mCherry-positive and CFP-negative cells (150 × 10^3 to 350 ×10^3 cells) were sorted by Flow Cytometry Core Lab at UMass Chan Medical School.

PCR and genotyping—Larvae from crosses between *gata2a*$^{+/um27}$ and *gata2a*$^{+/um345}$, with or without *cre* mRNA injection, individual embryos were separated by *cryaa:egfp* expression and subsequently genotyped for *gata2a*^{um27} using a KASP assay as previously (Biosearch Technologies)[18]. Excision of floxed exon 5 was determined by PCR using the following primers: 5'-TTAGAAGAACCGGTCTTCAGTATG-3' and 5'-GATCGCAGCCAAGCTTAACATTAAA-3'. *Gata2a*$^{i\Delta EC}$ larvae and embryos were identified using a KASP probe. For embryos from *foxc1a*$^{p162/um383}$ complementation cross, we first sorted embryos *cryaa:venus* expression at 3 dpf. Individual embryos were then genotyped for *foxc1a*^{p162} by KASP assay, as previously[18] and for deletion of *foxc1a* using PCR. Genotyping of *foxc1a*^{fl} was done by KASP assay. . Larvae from incrosses between *rasa1a*$^{+/um414}$; *rasa1b*$^{+/um290}$, with or without *cre* mRNA injection, individual embryos were separated by edema and/or *cryaa:egfp* expression at 4 dpf and subsequently genotyped for *rasa1b*^{um290} using KASP assays and deletion of exon 20 and exon 21 by PCR. Genotyping of *rasa1a*^{um414} or *rasa1a*^{um255} was done by KASP assay. All primer and KASP sequences can be found in Key Resources.

RT-qPCR—Total RNA was purified from Cre-injected or uninjected embryos (5 to 10 per sample) with TRIzol reagent (ThermoFisher). For *gata2a*, *foxc1a*, and *ruvbl1*, homozygous carriers of the floxed allele were incrossed, respectively, and used for RNA isolation. For embryos from an incross of *rasa1a*$^{+/um414}$ adults, we separated heads and tails of individuals at 3 dpf in Trizol and DNA lysis buffer, respectively. Individual DNAs were isolated and genotyped. After genotyping, individual RNAs from 5 embryos of matched genotype (*rasa1a*$^{+/+}$ or *rasa1a*$^{um414/um414}$) were pooled and subjected to qRT-PCR analysis. For FACS-isolated *mcherry+* cells (1.50–3.5×10^5) we used the Allprep DNA/RNA Micro kit (QIAGEN). cDNA was synthesized using 10ng of total RNA with SuperScript III First-Strand Synthesis SuperMix (ThermoFisher). For *foxc1a*, we removed residual genomic DNA before the reverse transcription reaction by treating with TURBO DNase (ThermoFisher). qPCR was performed with PowerSYBR Green PCR Master Mix (ThermoFisher) using ΔΔCT method on StepOne Plus Real-Time PCR machine (ThermoFisher). We used *eef1l1* for normalization. All primers for qRT-PCR are listed in the Key Resources Table.

Southern analysis—We purified genomic DNA from pooled embryos using the Blood & Cell Culture DNA Midi kit (QIAGEN). 5 or 10 μg of DNA was fully digested overnight with indicated restriction enzyme at the appropriate temperature. Digested samples were loaded onto a 0.7% agarose gel made with Tris acetate EDTA buffer alongside 100–200 ng of digoxigenin (DIG)-labeled DNA marker VII (MilliporeSigma) and run at 25V for 18 hours. After electrophoresis, the gel was sequentially incubated in 250 mM HCl for 25 minutes, 0.5M NaOH/1.5M NaCl for 45 minutes, and then 0.5M Tris pH7.5-HCl/1.5M NaCl for 30 minutes. Genomic DNA was then transferred from the gel to positively charged nylon membrane (MilliporeSigma) by standard capillary transfer overnight. Membrane was denatured on filter paper soaked in 0.4M NaOH for 5 minutes and UV-crosslinked at 420 × 10^2 μj/cm^2 in an XL-1000 UV CrossLinker (Spectronics Corp). Membranes were then prehybridized with DIG Easy Hyb solution (MilliporeSigma) in a HybriBag (Cosmo bio) at 42°C for 30 minutes with agitation. Prehybridization solution was replaced with fresh DIG Easy Hyb solution containing DIG labeled DNA probe at a final concentration between 50–100 ng/ml and incubated overnight at 42°C with agitation in a hybridization incubator (Robbins Scientific). An EGFP probe was PCR-amplified (5’-ATGGTGAGCAAGGGCGAGGAGCTG-3’ and 5’-ACTTGTACAGCTCGTCCATGCCG-3’) with DIG-labeled dNTP mix (MilliporeSigma) and AccuStart II DNA polymerase (Quantabio) using pBSIce-gata2aKI as a template followed by gel purification. Venus and mCherry fragments were PCR-amplified (*venus*:5’-ATGGTGAGCAAGGGCGAGGAGCTG-3’ and 5’-GGCGGCGGTCACGAACTCCAG-3’; *mcherry*: 5’-ATGGTGAGCAAGGGCGAGGAG-3’ and 5’-CTTACTTGTACAGCTCGTCCATG-3’) from pKHR8-foxc1aKI and separately subcloned into pJET2.1 (ThermoFisher) to give pJET-mVenus and -mCherry, respectively. DIG-labeled *venus* and *mcherry* DNA probes were then generated as above. Following hybridization, membranes were washed with 2x SSC/0.1% SDS at room temperature for 5 minutes, 0.5x SSC/0.1% SDS at 65°C for 20 minutes and 0.25x SSC/0.1% SDS at 65°C for 20 minutes, with agitation. After rinsing with maleic buffer (0.1M Maleic acid/150mM NaCl/0.3% Tween20-pH7.5), membrane was blocked in 1x Casein blocking

buffer (MilliporeSigma) diluted in maleic buffer at room temperature for 30 minutes and incubated with anti-DIG antibody conjugated with alkaline phosphatase (1:50,000 dilution; MilliporeSigma) in blocking buffer at room temperature for 30 minutes. Membranes were washed with maleic buffer at room temperature for 15 minutes twice, preactivated with 0.1M Tris-pH9.5/0.1M NaCl/50mM $MgCl_2$ then reacted with CDP-star ready-to-use substrate (MilliporeSigma). Chemiluminescence was detected by exposing membrane to film using CL-XPosure (ThermoFisher) or direct imaging on a ChemiDoc (Bio-rad).

***In situ* hybridization—**DNA templates for *urp1* or sst1.1. were generated by PCR as described elsewhere [19]. Following PCR, fragments were gel purified and then used as templates to generate DIG-labeled RNA probes using T3 polymerase. *In situ* hybridization was performed as previously described[59].

Imaging—Confocal imaging was performed using a LMS 710NLO (Zeiss) with ZEN10. Prior to imaging, larvae were subjected to lymphangiography using Qtracker 705 quantum dots as described previously [18]. Bright field and fluorescent images ware taken on M165FC (Leica) equipped with AxioCamMRc (Zeiss) using AxioVision SE64 Rel 4.9.1 software (Zeiss). Videos of blood circulation were acquired using differential interference contrast imaging on an Axioskop2 Plus (Zeiss) equipped with DMK21AU04 (IMAGINGSOURCE) using IC capture 2.5 software (IMAGINGSOURCE). Video files were saved as .mp4 and imported into Adobe Premiere Pro for labeling (Adobe). SEM sample preparation and image acquisition were performed as previously described[18].

QUANTIFICATION AND STATISTICAL ANALYSIS

All statistical tests were performed using Prism (GraphPad Software LLC), except Fishers Exact test, which was performed using the R software package. In all pairwise comparison, we tested for normal distribution using the Shapiro-Wilk test. All statistical tests applied in this study are noted in Figure legends. All error bars are mean with standard deviation.

Supplementary Material

Refer to Web version on PubMed Central for supplementary material.

ACKNOWLEDGEMENTS

This work was supported by NIH grants R35HL140017 and R21OD030004 to N. D. L. K.L. and S.A.W. were supported by NIH grants R01GM115911, R01HL150669, and 5F31HL147482. M. J. P. was supported by R01DK080730. We thank Sarah Oikemus for critical reading of the manuscript. The Burns Laboratory was supported by NIH grants R01HL139806 (C.G.B.) and R35HL135831 (C.E.B.).

INCLUSION AND DIVERSITY

We support inclusive, diverse, and equitable conduct of research.

REFERENCES

1. Beis D, and Stainier DY (2006). In vivo cell biology: following the zebrafish trend. Trends Cell Biol 16, 105–112. 10.1016/j.tcb.2005.12.001. [PubMed: 16406520]

2. Kimmel CB, Ballard WW, Kimmel SR, Ullmann B, and Schilling TF (1995). Stages of embryonic development of the zebrafish. Dev Dyn 203, 253–310. 10.1002/aja.1002030302. [PubMed: 8589427]

3. Mullins MC, Navajas Acedo J, Priya R, Solnica-Krezel L, and Wilson SW (2021). The zebrafish issue: 25 years on. Development 148. 10.1242/dev.200343.

4. Haffter P, Granato M, Brand M, Mullins MC, Hammerschmidt M, Kane DA, Odenthal J, van Eeden FJ, Jiang YJ, Heisenberg CP, et al. (1996). The identification of genes with unique and essential functions in the development of the zebrafish, Danio rerio. Development 123, 1–36. 10.1242/dev.123.1.1. [PubMed: 9007226]

5. Driever W, Solnica-Krezel L, Schier AF, Neuhauss SC, Malicki J, Stemple DL, Stainier DY, Zwartkruis F, Abdelilah S, Rangini Z, et al. (1996). A genetic screen for mutations affecting embryogenesis in zebrafish. Development 123, 37–46. 10.1242/dev.123.1.37. [PubMed: 9007227]

6. Hruscha A, Krawitz P, Rechenberg A, Heinrich V, Hecht J, Haass C, and Schmid B (2013). Efficient CRISPR/Cas9 genome editing with low off-target effects in zebrafish. Development 140, 4982–4987. 10.1242/dev.099085. [PubMed: 24257628]

7. Hwang WY, Fu Y, Reyon D, Maeder ML, Tsai SQ, Sander JD, Peterson RT, Yeh JR, and Joung JK (2013). Efficient genome editing in zebrafish using a CRISPR-Cas system. Nat Biotechnol 31, 227–229. 10.1038/nbt.2501. [PubMed: 23360964]

8. Johnson SL, and Weston JA (1995). Temperature-sensitive mutations that cause stage-specific defects in Zebrafish fin regeneration. Genetics 141, 1583–1595. 10.1093/genetics/141.4.1583. [PubMed: 8601496]

9. Carney TJ, and Mosimann C (2018). Switch and Trace: Recombinase Genetics in Zebrafish. Trends Genet 34, 362–378. 10.1016/j.tig.2018.01.004. [PubMed: 29429760]

10. Doetschman T, Gregg RG, Maeda N, Hooper ML, Melton DW, Thompson S, and Smithies O (1987). Targetted correction of a mutant HPRT gene in mouse embryonic stem cells. Nature 330, 576–578. 10.1038/330576a0. [PubMed: 3683574]

11. Thomas KR, and Capecchi MR (1987). Site-directed mutagenesis by gene targeting in mouse embryo-derived stem cells. Cell 51, 503–512. 10.1016/0092-8674(87)90646-5. [PubMed: 2822260]

12. Mansour SL, Thomas KR, and Capecchi MR (1988). Disruption of the proto-oncogene int-2 in mouse embryo-derived stem cells: a general strategy for targeting mutations to non-selectable genes. Nature 336, 348–352. 10.1038/336348a0. [PubMed: 3194019]

13. Gu H, Marth JD, Orban PC, Mossmann H, and Rajewsky K (1994). Deletion of a DNA polymerase beta gene segment in T cells using cell type-specific gene targeting. Science 265, 103–106. 10.1126/science.8016642. [PubMed: 8016642]

14. Nagy A (2000). Cre recombinase: the universal reagent for genome tailoring. Genesis 26, 99–109. [PubMed: 10686599]

15. Feil R, Brocard J, Mascrez B, LeMeur M, Metzger D, and Chambon P (1996). Ligand-activated site-specific recombination in mice. Proc Natl Acad Sci U S A 93, 10887–10890. 10.1073/pnas.93.20.10887. [PubMed: 8855277]

16. Burg L, Palmer N, Kikhi K, Miroshnik ES, Rueckert H, Gaddy E, MacPherson Cunningham C, Mattonet K, Lai SL, Marin-Juez R, et al. (2018). Conditional mutagenesis by oligonucleotide-mediated integration of loxP sites in zebrafish. PLoS Genet 14, e1007754. 10.1371/journal.pgen.1007754. [PubMed: 30427827]

17. Hoshijima K, Jurynec MJ, and Grunwald DJ (2016). Precise Editing of the Zebrafish Genome Made Simple and Efficient. Dev Cell 36, 654–667. 10.1016/j.devcel.2016.02.015. [PubMed: 27003937]

18. Shin M, Nozaki T, Idrizi F, Isogai S, Ogasawara K, Ishida K, Yuge S, Roscoe B, Wolfe SA, Fukuhara S, et al. (2019). Valves Are a Conserved Feature of the Zebrafish Lymphatic System. Dev Cell. 10.1016/j.devcel.2019.08.019.

19. Andrzejczuk LA, Banerjee S, England SJ, Voufo C, Kamara K, and Lewis KE (2018). Tal1, Gata2a, and Gata3 Have Distinct Functions in the Development of V2b and Cerebrospinal Fluid-Contacting KA Spinal Neurons. Front Neurosci 12, 170. 10.3389/fnins.2018.00170. [PubMed: 29651232]

20. Pase L, Layton JE, Kloosterman WP, Carradice D, Waterhouse PM, and Lieschke GJ (2009). miR-451 regulates zebrafish erythroid maturation in vivo via its target gata2. Blood 113, 1794–1804. 10.1182/blood-2008-05-155812. [PubMed: 18849488]
21. Kurita R, Sagara H, Aoki Y, Link BA, Arai K, and Watanabe S (2003). Suppression of lens growth by alphaA-crystallin promoter-driven expression of diphtheria toxin results in disruption of retinal cell organization in zebrafish. Dev Biol 255, 113–127. 10.1016/s0012-1606(02)00079-9. [PubMed: 12618137]
22. Martin DI, and Orkin SH (1990). Transcriptional activation and DNA binding by the erythroid factor GF-1/NF-E1/Eryf 1. Genes & development 4, 1886–1898. 10.1101/gad.4.11.1886. [PubMed: 2276623]
23. Charles MA, Saunders TL, Wood WM, Owens K, Parlow AF, Camper SA, Ridgway EC, and Gordon DF (2006). Pituitary-specific Gata2 knockout: effects on gonadotrope and thyrotrope function. Mol Endocrinol 20, 1366–1377. 10.1210/me.2005-0378. [PubMed: 16543408]
24. Zhu C, Smith T, McNulty J, Rayla AL, Lakshmanan A, Siekmann AF, Buffardi M, Meng X, Shin J, Padmanabhan A, et al. (2011). Evaluation and application of modularly assembled zinc-finger nucleases in zebrafish. Development 138, 4555–4564. 10.1242/dev.066779. [PubMed: 21937602]
25. Topczewska JM, Topczewski J, Solnica-Krezel L, and Hogan BL (2001). Sequence and expression of zebrafish foxc1a and foxc1b, encoding conserved forkhead/winged helix transcription factors. Mech Dev 100, 343–347. 10.1016/s0925-4773(00)00534-7. [PubMed: 11165495]
26. Baranasic D, Hortenhuber M, Balwierz PJ, Zehnder T, Mukarram AK, Nepal C, Varnai C, Hadzhiev Y, Jimenez-Gonzalez A, Li N, et al. (2022). Multiomic atlas with functional stratification and developmental dynamics of zebrafish cis-regulatory elements. Nat Genet 54, 1037–1050. 10.1038/s41588-022-01089-w. [PubMed: 35789323]
27. Shahbazi R, Sghia-Hughes G, Reid JL, Kubek S, Haworth KG, Humbert O, Kiem HP, and Adair JE (2019). Targeted homology-directed repair in blood stem and progenitor cells with CRISPR nanoformulations. Nat Mater 18, 1124–1132. 10.1038/s41563-019-0385-5. [PubMed: 31133730]
28. Moreno-Mateos MA, Fernandez JP, Rouet R, Vejnar CE, Lane MA, Mis E, Khokha MK, Doudna JA, and Giraldez AJ (2017). CRISPR-Cpf1 mediates efficient homology-directed repair and temperature-controlled genome editing. Nat Commun 8, 2024. 10.1038/s41467-017-01836-2. [PubMed: 29222508]
29. Huang CJ, Tu CT, Hsiao CD, Hsieh FJ, and Tsai HJ (2003). Germ-line transmission of a myocardium-specific GFP transgene reveals critical regulatory elements in the cardiac myosin light chain 2 promoter of zebrafish. Dev Dyn 228, 30–40. 10.1002/dvdy.10356. [PubMed: 12950077]
30. Banerjee S, Hayer K, Hogenesch JB, and Granato M (2015). Zebrafish foxc1a drives appendage-specific neural circuit development. Development 142, 753–762. 10.1242/dev.115816. [PubMed: 25670796]
31. Ferre-Fernandez JJ, Sorokina EA, Thompson S, Collery RF, Nordquist E, Lincoln J, and Semina EV (2020). Disruption of foxc1 genes in zebrafish results in dosage-dependent phenotypes overlapping Axenfeld-Rieger syndrome. Hum Mol Genet 29, 2723–2735. 10.1093/hmg/ddaa163. [PubMed: 32720677]
32. Mao YQ, and Houry WA (2017). The Role of Pontin and Reptin in Cellular Physiology and Cancer Etiology. Front Mol Biosci 4, 58. 10.3389/fmolb.2017.00058. [PubMed: 28884116]
33. Li Y, Zhao L, Yuan S, Zhang J, and Sun Z (2017). Axonemal dynein assembly requires the R2TP complex component Pontin. Development 144, 4684–4693. 10.1242/dev.152314. [PubMed: 29113992]
34. Trahey M, and McCormick F (1987). A cytoplasmic protein stimulates normal N-ras p21 GTPase, but does not affect oncogenic mutants. Science 238, 542–545. 10.1126/science.2821624. [PubMed: 2821624]
35. Eerola I, Boon LM, Mulliken JB, Burrows PE, Dompmartin A, Watanabe S, Vanwijck R, and Vikkula M (2003). Capillary malformation-arteriovenous malformation, a new clinical and genetic disorder caused by RASA1 mutations. Am J Hum Genet 73, 1240–1249. 10.1086/379793. [PubMed: 14639529]

36. Henkemeyer M, Rossi DJ, Holmyard DP, Puri MC, Mbamalu G, Harpal K, Shih TS, Jacks T, and Pawson T (1995). Vascular system defects and neuronal apoptosis in mice lacking ras GTPase-activating protein. Nature 377, 695–701. 10.1038/377695a0. [PubMed: 7477259]
37. Lapinski PE, Kwon S, Lubeck BA, Wilkinson JE, Srinivasan RS, Sevick-Muraca E, and King PD (2012). RASA1 maintains the lymphatic vasculature in a quiescent functional state in mice. J Clin Invest 122, 733–747. 10.1172/JCI46116. [PubMed: 22232212]
38. Meyerhans A, Vartanian JP, and Wain-Hobson S (1990). DNA recombination during PCR. Nucleic Acids Res 18, 1687–1691. 10.1093/nar/18.7.1687. [PubMed: 2186361]
39. Won M, and Dawid IB (2017). PCR artifact in testing for homologous recombination in genomic editing in zebrafish. PLoS One 12, e0172802. 10.1371/journal.pone.0172802. [PubMed: 28362803]
40. Zhang D, Gates KP, Barske L, Wang G, Lancman JJ, Zeng XI, Groff M, Wang K, Parsons MJ, Crump JG, and Dong PDS (2017). Endoderm Jagged induces liver and pancreas duct lineage in zebrafish. Nat Commun 8, 769. 10.1038/s41467-017-00666-6. [PubMed: 28974684]
41. Balik-Meisner M, Truong L, Scholl EH, Tanguay RL, and Reif DM (2018). Population genetic diversity in zebrafish lines. Mamm Genome 29, 90–100. 10.1007/s00335-018-9735-x. [PubMed: 29368091]
42. Butler MG, Iben JR, Marsden KC, Epstein JA, Granato M, and Weinstein BM (2015). SNPfisher: tools for probing genetic variation in laboratory-reared zebrafish. Development 142, 1542–1552. 10.1242/dev.118786. [PubMed: 25813542]
43. Deng C, and Capecchi MR (1992). Reexamination of gene targeting frequency as a function of the extent of homology between the targeting vector and the target locus. Mol Cell Biol 12, 3365–3371. 10.1128/mcb.12.8.3365-3371.1992. [PubMed: 1321331]
44. Zetsche B, Gootenberg JS, Abudayyeh OO, Slaymaker IM, Makarova KS, Essletzbichler P, Volz SE, Joung J, van der Oost J, Regev A, et al. (2015). Cpf1 is a single RNA-guided endonuclease of a class 2 CRISPR-Cas system. Cell 163, 759–771. 10.1016/j.cell.2015.09.038. [PubMed: 26422227]
45. Sabine A, Agalarov Y, Maby-El Hajjami H, Jaquet M, Hagerling R, Pollmann C, Bebber D, Pfenniger A, Miura N, Dormond O, et al. (2012). Mechanotransduction, PROX1, and FOXC2 cooperate to control connexin37 and calcineurin during lymphatic-valve formation. Dev Cell 22, 430–445. 10.1016/j.devcel.2011.12.020. [PubMed: 22306086]
46. Kazenwadel J, Betterman KL, Chong CE, Stokes PH, Lee YK, Secker GA, Agalarov Y, Demir CS, Lawrence DM, Sutton DL, et al. (2015). GATA2 is required for lymphatic vessel valve development and maintenance. J Clin Invest 125, 2979–2994. 10.1172/JCI78888. [PubMed: 26214525]
47. Wierson WA, Welker JM, Almeida MP, Mann CM, Webster DA, Torrie ME, Weiss TJ, Kambakam S, Vollbrecht MK, Lan M, et al. (2020). Efficient targeted integration directed by short homology in zebrafish and mammalian cells. Elife 9. 10.7554/eLife.53968.
48. Sugimoto K, Hui SP, Sheng DZ, and Kikuchi K (2017). Dissection of zebrafish shha function using site-specific targeting with a Cre-dependent genetic switch. Elife 6. 10.7554/eLife.24635.
49. Li W, Zhang Y, Han B, Li L, Li M, Lu X, Chen C, Lu M, Zhang Y, Jia X, et al. (2019). One-step efficient generation of dual-function conditional knockout and geno-tagging alleles in zebrafish. Elife 8. 10.7554/eLife.48081.
50. Liu F, Kambakam S, Almeida MP, Ming Z, Welker JM, Wierson WA, SchultzRogers LE, Ekker SC, Clark KJ, Essner JJ, and McGrail M (2022). Cre/lox regulated conditional rescue and inactivation with zebrafish UFlip alleles generated by CRISPR-Cas9 targeted integration. Elife 11. 10.7554/eLife.71478.
51. Ghanta KS, Chen Z, Mir A, Dokshin GA, Krishnamurthy PM, Yoon Y, Gallant J, Xu P, Zhang XO, Ozturk A, et al. (2021). 5′ modifications improve potency and efficacy of dna donors for precision genome editing. eLife 10, e72216. 10.7554/eLife.72216. [PubMed: 34665130]
52. Moore JC, Sheppard-Tindell S, Shestopalov IA, Yamazoe S, Chen JK, and Lawson ND (2013). Post-transcriptional mechanisms contribute to Etv2 repression during vascular development. Dev Biol 384, 128–140. 10.1016/j.ydbio.2013.08.028. [PubMed: 24036310]

53. Villefranc JA, Amigo J, and Lawson ND (2007). Gateway compatible vectors for analysis of gene function in the zebrafish. Dev Dyn 236, 3077–3087. 10.1002/dvdy.21354. [PubMed: 17948311]

54. Kwan KM, Fujimoto E, Grabher C, Mangum BD, Hardy ME, Campbell DS, Parant JM, Yost HJ, Kanki JP, and Chien CB (2007). The Tol2kit: a multisite gateway-based construction kit for Tol2 transposon transgenesis constructs. Dev Dyn 236, 3088–3099. 10.1002/dvdy.21343. [PubMed: 17937395]

55. Shin M, Male I, Beane TJ, Villefranc JA, Kok FO, Zhu LJ, and Lawson ND (2016). Vegfc acts through ERK to induce sprouting and differentiation of trunk lymphatic progenitors. Development 143, 3785–3795. 10.1242/dev.137901. [PubMed: 27621059]

56. Mosimann C, Kaufman CK, Li P, Pugach EK, Tamplin OJ, and Zon LI (2011). Ubiquitous transgene expression and Cre-based recombination driven by the ubiquitin promoter in zebrafish. Development 138, 169–177. 10.1242/dev.059345. [PubMed: 21138979]

57. Liu P, Luk K, Shin M, Idrizi F, Kwok S, Roscoe B, Mintzer E, Suresh S, Morrison K, Frazao JB, et al. (2019). Enhanced Cas12a editing in mammalian cells and zebrafish. Nucleic Acids Res 47, 4169–4180. 10.1093/nar/gkz184. [PubMed: 30892626]

58. Wu Y, Zeng J, Roscoe BP, Liu P, Yao Q, Lazzarotto CR, Clement K, Cole MA, Luk K, Baricordi C, et al. (2019). Highly efficient therapeutic gene editing of human hematopoietic stem cells. Nat Med 25, 776–783. 10.1038/s41591-019-0401-y. [PubMed: 30911135]

59. Hauptmann G, and Gerster T (1994). Two-color whole-mount in situ hybridization to vertebrate and Drosophila embryos. Trends Genet 10, 266. [PubMed: 7940754]

Highlights

- Improved methods for generating conditional deletion alleles in zebrafish
- Generation of four zebrafish lines bearing endogenously floxed alleles
- Blueprint for characterization and validation of floxed alleles in zebrafish
- Use of a floxed allele to define cell-specific gene function in zebrafish

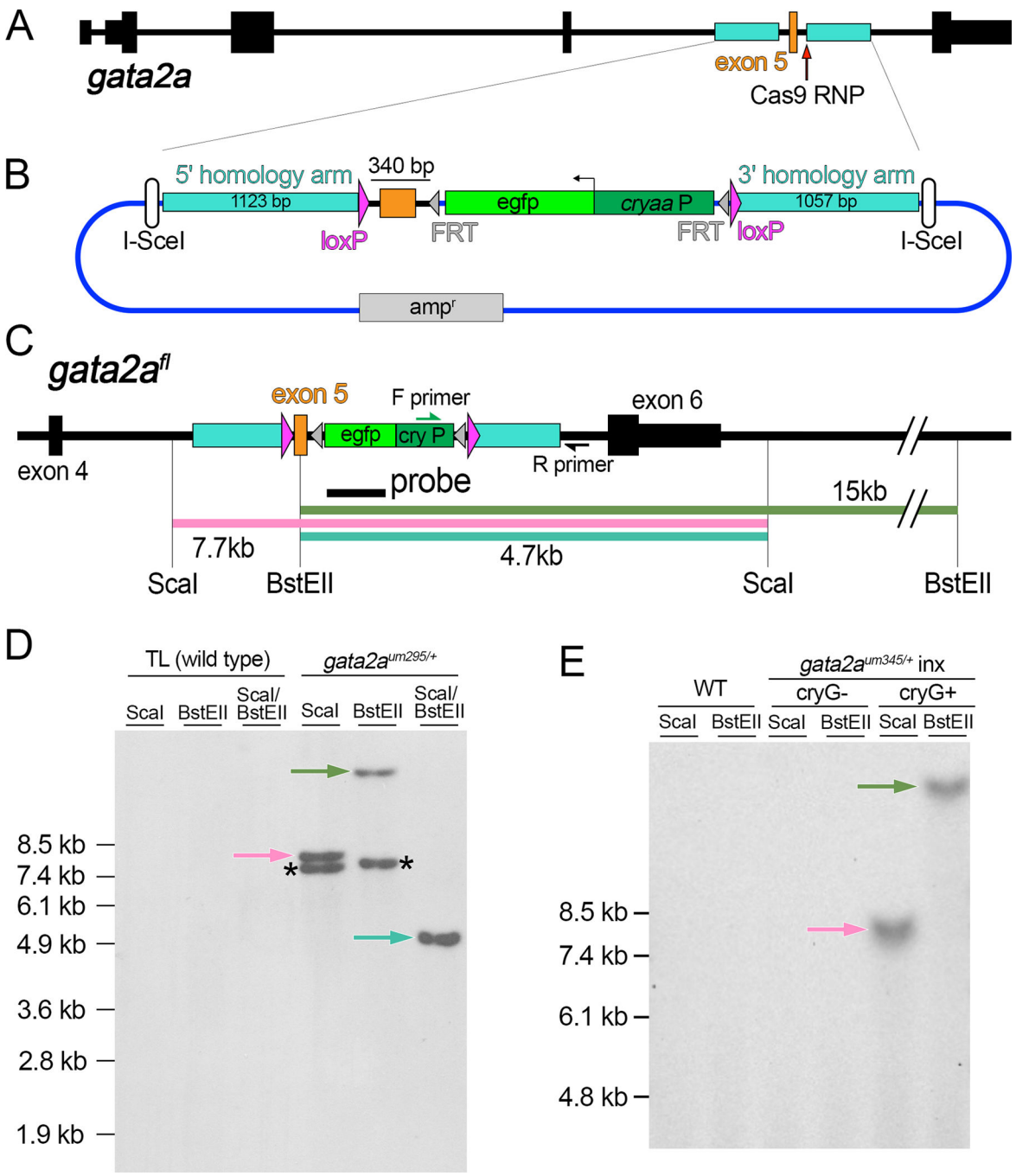

Figure 1. Generation of a *gata2a* conditional deletion allele.

(A) Zebrafish *gata2a* locus. (B) Targeting plasmid for floxed *gata2a* allele. egfp – enhanced green fluorescent protein, cryaa:P – cryaa promoter element, *amp*^{r} – ampicillin resistance cassette. (C) Restriction map of *gata2a*^{fl}. PCR primers and probe are shown. (D, E) Southern analysis of embryos of indicated genotype. Blots hybridized with a DIG-labeled *egfp* probe detected by chemiluminescence. Arrows denote fragments expected from precise integration, asterisked fragments from random integration.

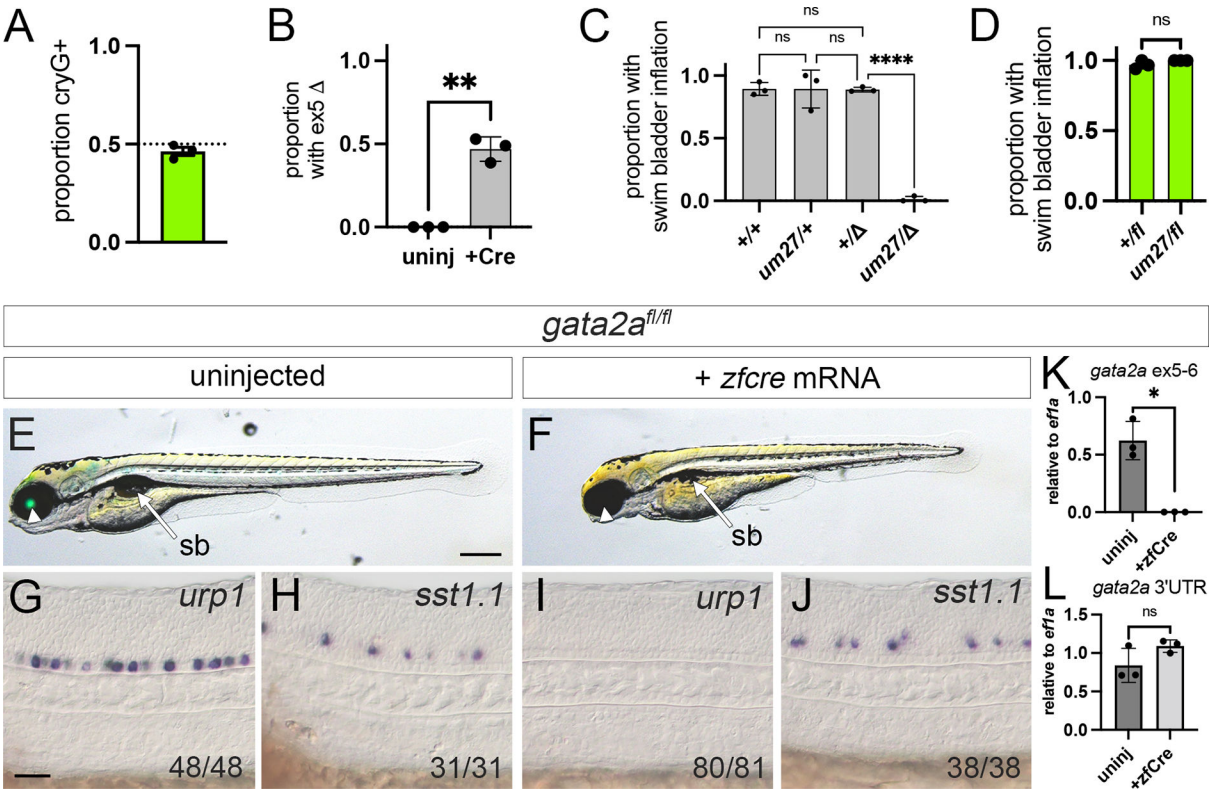

Figure 2. Functional validation of a floxed *gata2a* allele.

(A-D) Embryos from crosses between *gata2a*$^{+/um27}$ and *gata2a*$^{+/fl}$ individuals (n = 3 clutches). (A) Proportion of embryos expressing lens *Egfp* (cryG+) at 2 dpf. (B) Proportion of uninjected or *cre* mRNA-injected embryos with exon 5 deletion. ** p<0.01, paired t-test. (C) Proportion of embryos of indicated genotype with inflated swim bladder (sb) following *cre* mRNA injection. "Δ" denotes exon 5 deletion confirmed by PCR. Analysis of variance, p<0.0001. **** p<0.0001, Tukey's multiple comparison test. (D) Proportion of uninjected *cryaa:egfp*-positive embryos of indicated genotype with inflated swim bladder at 5 dpf. ns – not significant, Wilcoxon test. (E-J) Homozygous *gata2a*$^{fl/fl}$ (E, F) larvae at 5 dpf or (G-J) embryos at 24 hpf. Lateral views, anterior to the left, dorsal is up. (E, G, H) Uninjected or (F, I, J) injected with *zfcre* mRNA at 1-cell stage. (E, F) Overlay of transmitted light and green fluorescence at 5 dpf. Arrowhead denotes lens Egfp expression, or absence thereof, arrow indicates sb. Scale bar is 250 μm. (G-J) Differential interference contrast (DIC) images of 24 hpf embryos following whole mount in situ hybridization with antisense riboprobes against indicated transcript. Scale bar is 50 μm. (K, L) Quantitative RT-PCR of uninjected or *zfcre* mRNA-injected *gata2a*$^{fl/fl}$ embryos at 24 hpf for *gata2a* transcript with (K) exon 5 and 6, or (L) 3' UTR. Paired t-test, * - p<0.05, ns – not statistically significant.

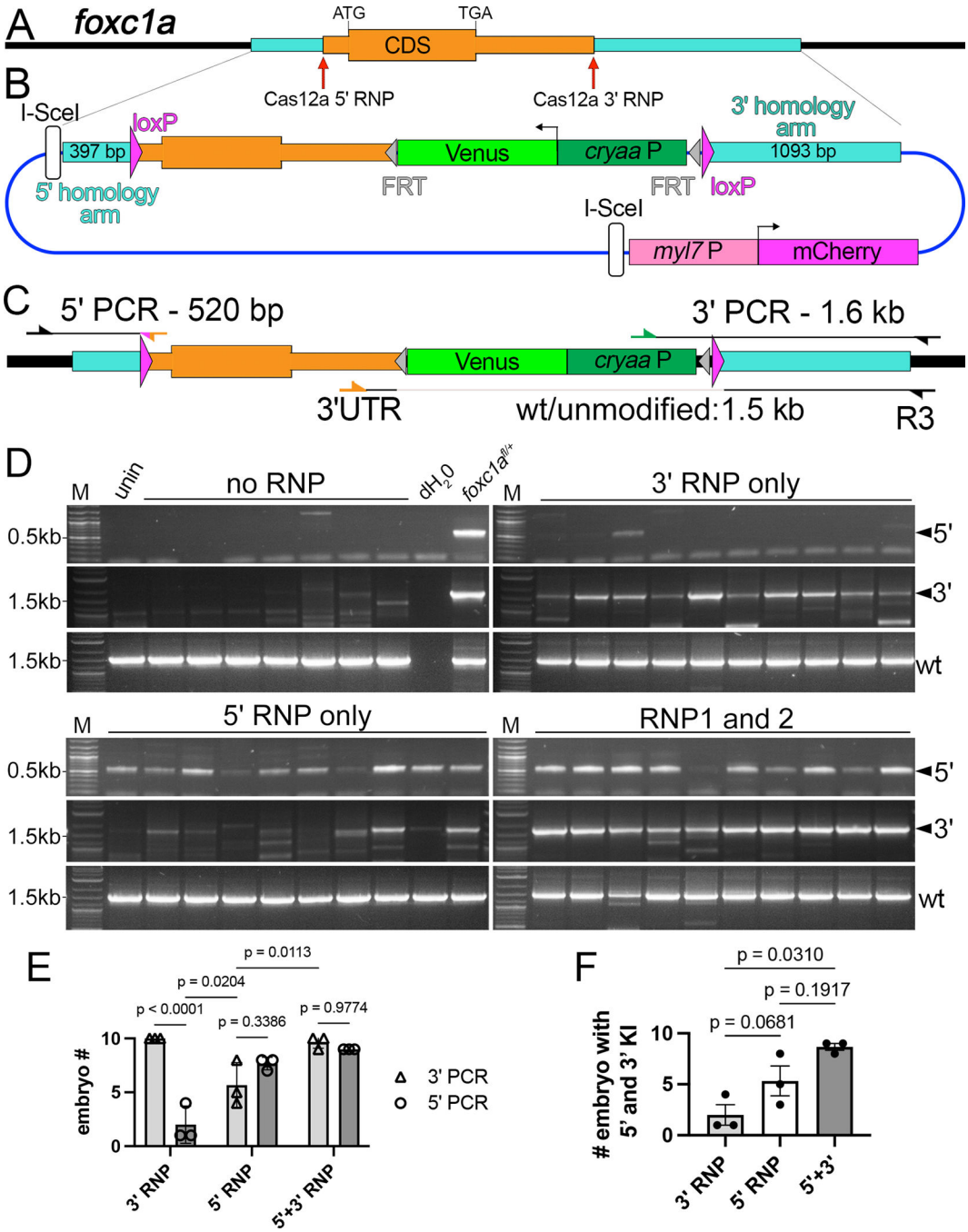

Figure 3. Dual CRISPR targeting improves complete knock-in of a floxed cassette.

(A) Zebrafish *foxc1a* locus; Homology arms (turquoise) and Cas12a ribonucleoprotein (RNP) targets indicated, as are coding sequence (CDS), start (ATG) and stop codons (TGA). (B) Targeting plasmid for *foxc1a*. *cryaaP* – *cryaa* promoter. Not to scale as *myl7:mcherry* cassette is immediately adjacent to the 3' homology arm; see Supplementary File S2. (C) *Fox1a*^{fl} locus with PCR primer locations indicated. (D) 5' and 3' junction PCRs from 2 dpf Venus/mCherry-positive individual embryos injected with indicated RNPs. (E) Number of embryos injected with indicated RNP showing either 5' and 3' knock-in. One-way ANOVA,

p=0.0114; Holm-Sidak multiple comparison test, p-values indicated. (F) Number of embryos injected with indicated RNP(s) with both 5’ and 3’ knock-in. Tukey’s multiple comparison test, p-values shown (E,F) Each point is a replicate from 10 normal embryos.

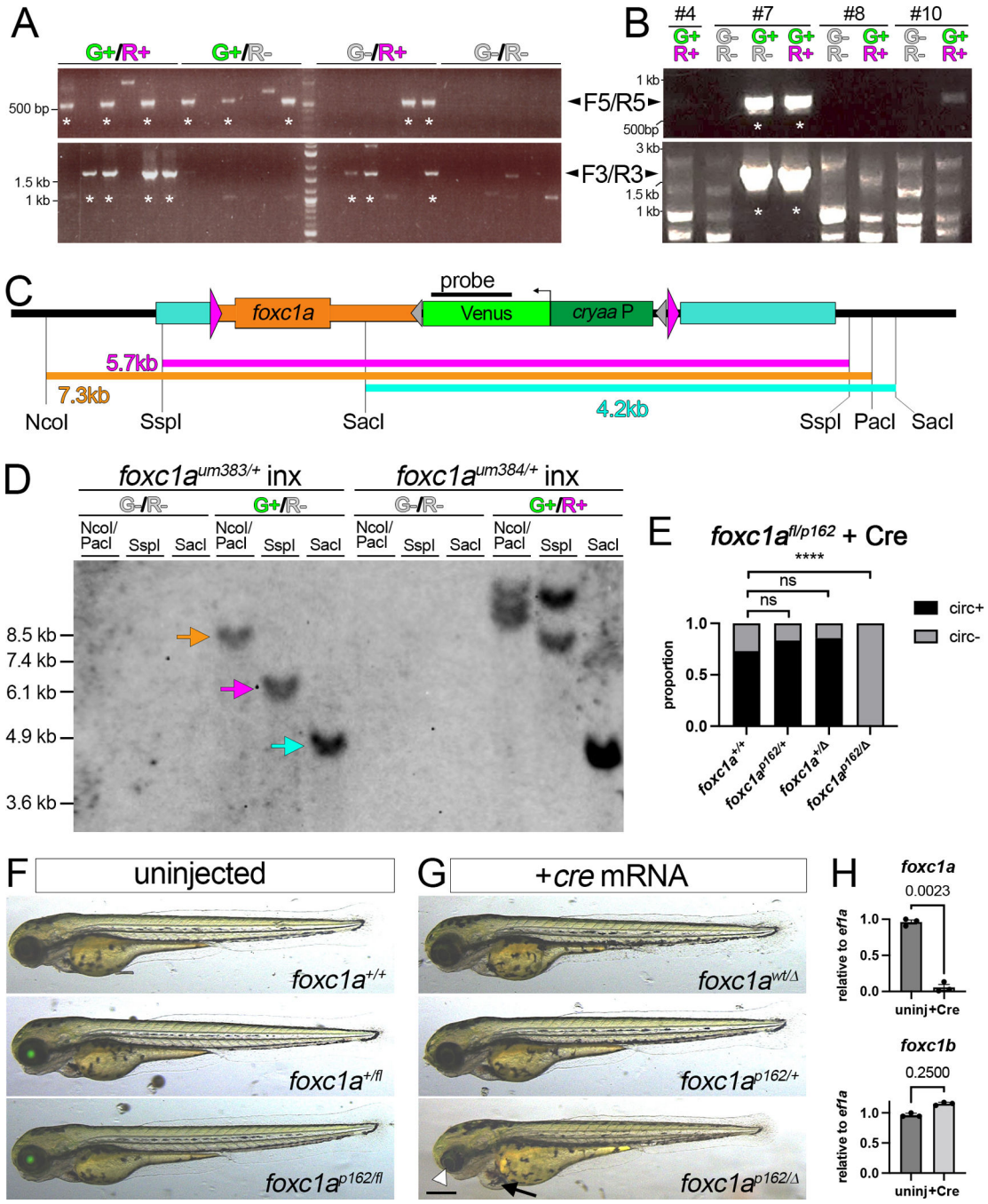

Figure 4. Generation of *foxc1a*^{fl} using transgenic counter-screening

(A, B) PCR of 3 dpf embryos scored for Venus (G+) and mCherry (R+) expression with indicated primer pairs (F5/R5 or F3/R3, see Figure 3C). Asterisk denotes lanes with expected size. (A) Individual embryos injected with Cas12a RNPs, targeting construct, and I-SceI. (B) Pooled F1 embryos from indicated founder. (C) *Foxc1a*^{fl} restriction map. (D) Southern analysis of F2 embryos of indicated genotype screened for Venus ("G") or mCherry ("R") expression. Blot hybridized with DIG-labeled *venus* probe detected by chemiluminescence. (E) Proportion of 3 dpf larvae of indicated genotype with or without

circulation. Total embryos: *foxc1a*$^{+/+}$ - 26, *foxc1*$^{p162/+}$ - 12, *foxc1a*$^{+/\Delta}$ - 14, *foxc1a*$^{p162/\Delta}$ - 16. Fisher's exact test, ****p<0.0001. (F, G) Overlay of transmitted light and green fluorescence at 3 dpf. Larvae from cross between *foxc1a*$^{+/fl}$ and *foxc1a*$^{+/p162}$ carriers. (F) Uninjected embryos of indicated genotype with normal morphology. (G) Embryos injected with *cre* mRNA. Arrowhead denotes small eye and arrow indicates cardiac edema (*bottom*). (F, G) Scale bar is 250 μm. (H) Quantitative RT-PCR for *foxc1a* and *foxc1b* in *foxc1a*$^{fl/fl}$ embryos. Embryos left uninjected or injected with *zfcre* mRNA at 1-cell stage. Paired t-test, p values are shown.

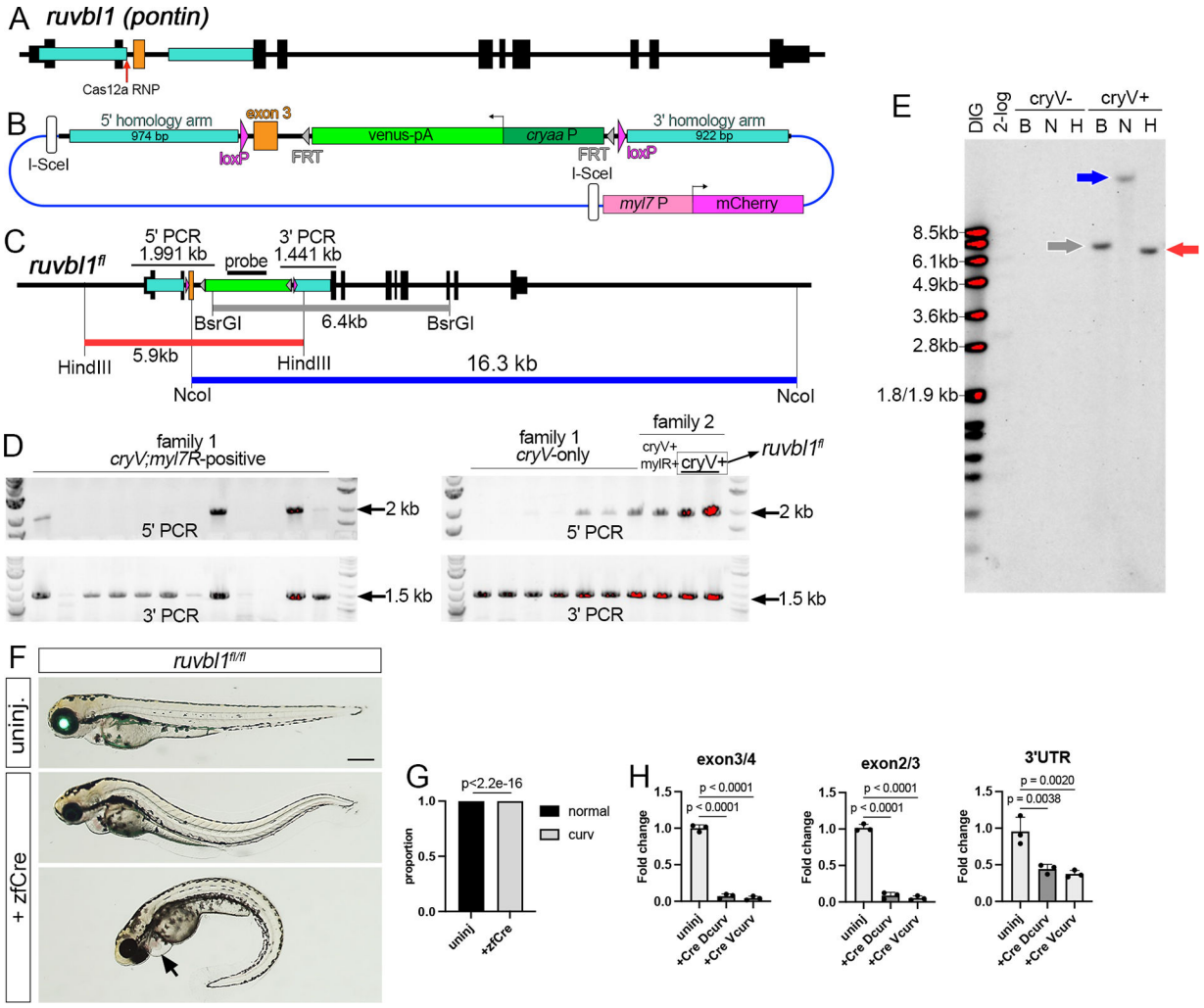

Figure 5. A floxed *ruvbl1* allele (*ruvbl1*^{fl}).

(A) *Ruvbl1* locus. (B) *Ruvbl1*^{fl} targeting construct. (C) *Ruvbl1*^{fl} restriction map. 5' and 3' PCR screening fragments indicated. (D) PCR of individual F1 embryos from group family P0 incrosses. cryV denotes Venus expression, myl7R is mCherry expression. Family 2 founder transmitting cryV-only embryos (boxed) was identified by individual outcross. (E) Southern analysis of F2 cryV-positive and -negative siblings from outcross of F1 *ruvbl1*$^{fl/+}$ carriers (B – BsrGI, N – NcoI, H – HindIII). Blot hybridized with DIG-labeled *venus* probe detected using chemiluminescence. (F) *Ruvbl1*$^{fl/fl}$ larvae at 3 dpf; Lateral views, anterior to the left, dorsal is up. Overlays of epifluorescent and transmitted light images. *Top panel*, uninjected embryo expressing *cryaa:venus*. *Bottom panels*, embryos injected with *zfcre* mRNA showing dorsal (*middle*) or ventral (*bottom*) trunk curvature, cardiac edema (indicated by arrow), and loss of *cryaa:venus*. Scale bar is 250 μm. (G) Trunk curvature penetrance in uninjected (n=113) or *zfcre*-injected (n=379) *ruvbl1*$^{fl/fl}$ larvae. Fishers exact test. (H) qRTPCR across indicated exon junctions or in 3' UTR. Dunnett's multiple comparison test, p-values shown.

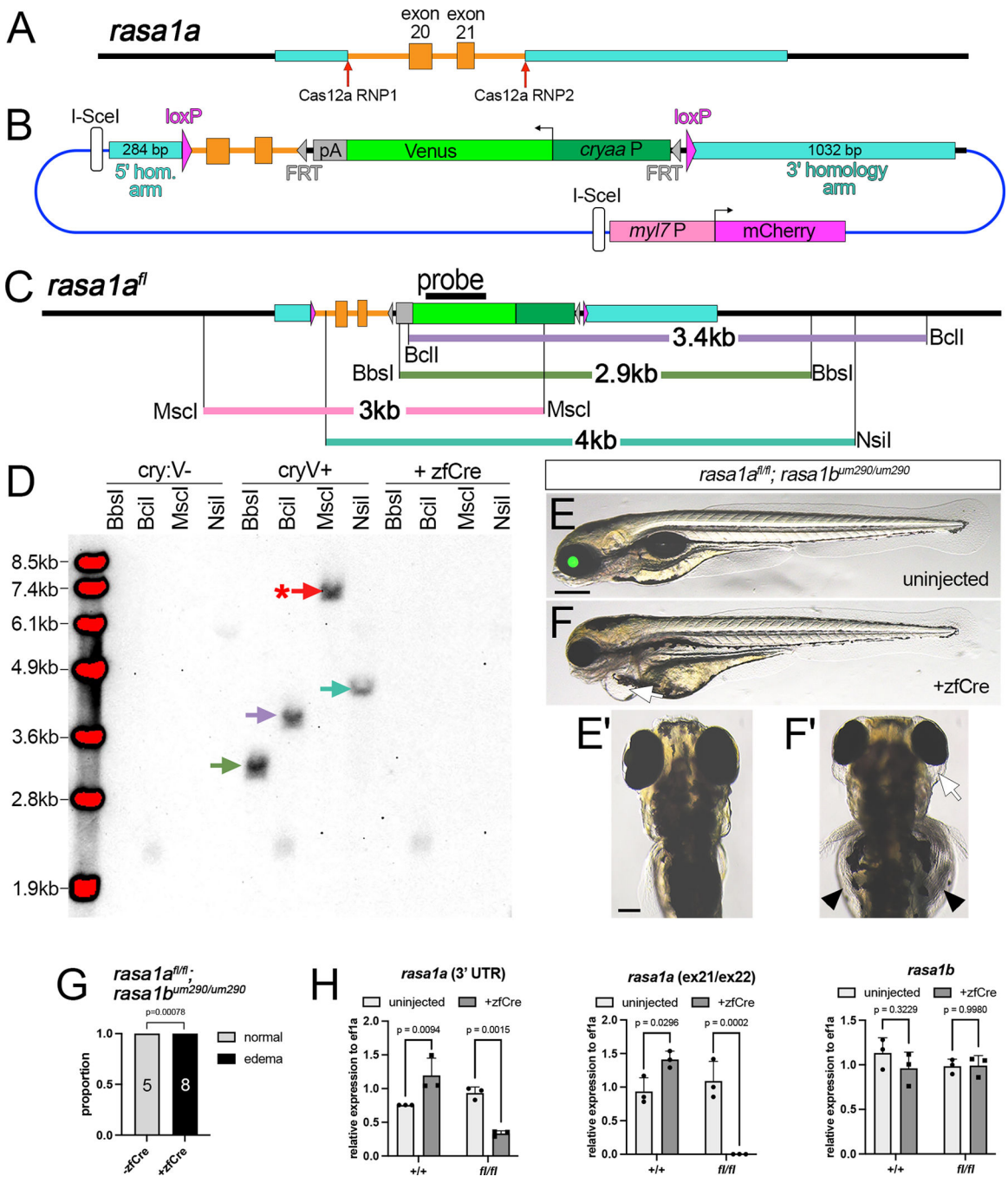

Figure 6. A floxed *rasa1a* allele (*rasa1a*^{fl})

(A) *Rasa1a* exons 20 and 21. (B) *Rasa1*^{fl} targeting construct. (C) *Rasa1a*^{fl} restriction map. (D) Southern analysis of F1 *cryaa:venus*-positive and -negative siblings, or those injected with zfCre mRNA. Blot hybridized with DIG-labeled *venus* probe detected using chemiluminescence. Asterisk denotes larger fragment than expected. (E, F) *rasa1a*$^{fl/fl}$;*rasa1b*$^{um290/um290}$ larvae at 4 dpf. Scale bar, 250 μm. (E, E') Uninjected larva; lateral and dorsal views, respectively. (F) Lateral view of larva injected with *zfcre* mRNA showing cardiac edema (arrow). (F') Dorsal view of larva in (F) showing ocular (arrow)

and gut edema (arrowhead). (E', F') Scale bar, 100 μm. (G) Penetrance of edema in 4 dpf larvae of indicated genotype. Fisher's exact test, p-values shown. (H) qRT-PCR for indicated transcript in uninjected or *zfcre*-injected embryos of indicated genotype. Sidak's multiple comparison test, p-values shown.

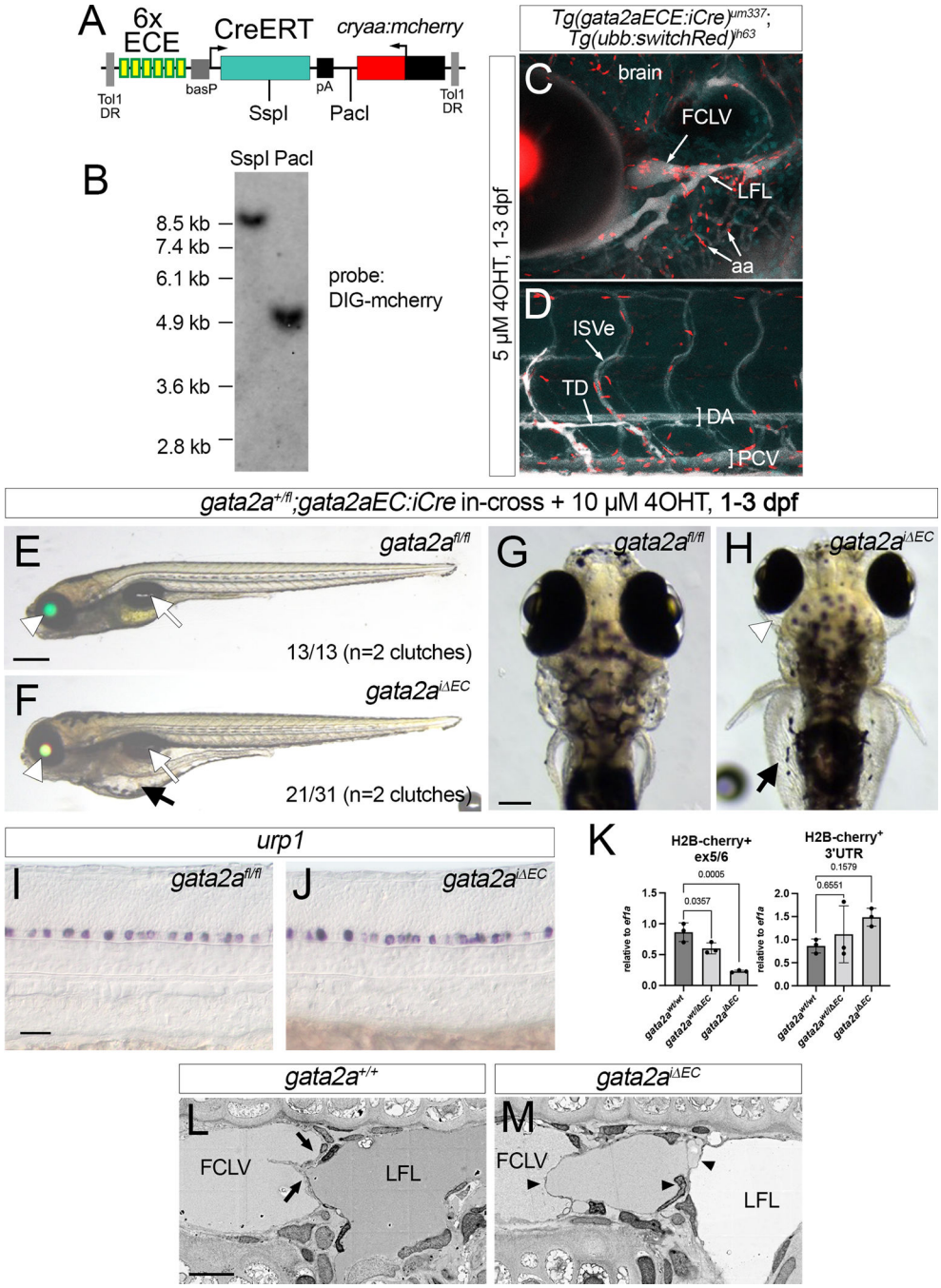

Figure 7. Endothelial *gata2a* is required for lymphatic valve function and formation.

(A) Restriction map of Tol1 *gata2aECE:iCre* transgene. (B) Southern analysis of *Tg(gata2aECE:iCre)*^{um337} embryos. Blot hybridized with a DIG-labeled *mcherry* probe detected by chemiluminescence. (C, D) Confocal micrograph overlays of *Tg(gata2aECE:iCre)*^{um337}*; (ubb:switchRed)*^{jh63} 7 dpf larvae showing expression of H2B-Cherry (red), cerulean (blue) and Qtracker705 introduced via lymphangiography (white). Lateral views, anterior to the left, dorsal is up. (C) Cranial vessels; (D) trunk vessels. FCLV – facial collecting lymphatic vessel, LFL – lateral facial lymphatic vessel, aa – aortic arch

blood vessels, ISVe – intersomitic vein, TD – thoracic duct, DA – dorsal aorta, PCV – posterior cardinal vein. (E, F) 6 dpf and (G, H) 7 dpf larvae from indicated cross with 10μM 4OHT treatment from 1 dpf to 3 dpf. (G, H) Scale bar, 100 μm. (E, G) *gata2a*$^{fl/fl}$ larvae without iCre. (F, H) *gata2a*$^{fl/fl}$*; Tg(gata2aEC:iCre)*^{um337} larvae, referred to as *gata2a*$^{i\Delta EC}$. (E, F) Transmitted light, green and red fluorescence overlay. White arrowhead denotes lens, white arrow inflated swim bladder. Scale bar, 250 μm. (F, H) Black arrows indicate gut edema. (H) White arrowhead indicates ocular edema. (I, J) *Urp1* expression by whole mount *in situ* hybridization in 24 hpf embryos of indicated genotype treated with 5 μM 4OHT from 6 hpf. Scale bar, 50 μm. (K) Quantitative RT-PCR for *gata2a* exon 5/6 or 3' UTR from H2B-mcherry-positive cells from *gata2a*$^{i\Delta EC}$*;ubi:switchRed* at 5 dpf and 6 dpf treated with 5 μM 4OHT from 6 hpf to 4 dpf. Exon 5/6, analysis of variance, $p<0.005$; for 3', not significant. Pairwise comparisons performed using Dunnett's multiple comparison test, p values indicated. (L, M) Scanning electron micrographs of lymphatic valves in 7 dpf larvae of indicated genotype following 5 μM 4OHT from 1 dpf to 3 dpf. Lateral views, dorsal is up, anterior to the left. Normal bicuspid valve leaflets indicated (arrows). Multiple abnormal leaflets (black arrowheads) appear in *gata2a*$^{i\Delta EC}$ larvae. FCLV – facial collecting lymphatic vessel. LFL – lateral facial lymphatic vessel. Scale bar, 5 μm.

KEY RESOURCES TABLE

REAGENT or RESOURCE	SOURCE	IDENTIFIER
Antibodies		
Anti-Digoxigenin-AP, Fab fragments	MilliporeSigma	11093274910
Chemicals, peptides, and recombinant proteins		
2×Super Pfx MasterMix	Cowin Biotech	CW2965F
Gateway™ LR Clonase™ II Enzyme mix	ThermoFisher Scientific	11791020
KAPA2G Fast HotStart ReadyMix	KAPA Biosystems	7961235001
AccuStart II DNA polymerase	Quantabio	95141
PowerSYBR Green PCR Master Mix	ThermoFisher Scientific	4367659
SuperScript™ III First-Strand Synthesis SuperMix	ThermoFisher Scientific	18080400
TURBO™ DNase	ThermoFisher Scientific	AM2238
PACE 2x Genotyping Master Mix High ROX 500nM	3Cr Biosciences	001-0010
ISceI	New England Biolabs	R0694
ClaI	New England Biolabs	R0197
SacII	New England Biolabs	R0157
XhoI	New England Biolabs	R0146
NotI-HF	New England Biolabs	R3189
HindIII-HF	New England Biolabs	R3104
EcoRI-HF	New England Biolabs	R3101
ScaI-HF	New England Biolabs	R3122
BstEII-HF	New England Biolabs	R3162
NcoI-HF	New England Biolabs	R3193
PacI	New England Biolabs	R0547
SspI-HF	New England Biolabs	R0132
BbsI-HF	New England Biolabs	R3539
BclI-HF	New England Biolabs	R3160
MscI	New England Biolabs	R0534
NsiI-HF	New England Biolabs	R3127
BsrGI-HF	New England Biolabs	R3575
BamHI-HF	New England Biolabs	R3136
SalI-HF	New England Biolabs	R3138
(Z)-4-Hydroxytamoxifen	MilliporeSigma	H7904
DIG-labeled DNA marker VII	MilliporeSigma	11669940910
DIG Easy Hyb™ Granules	MilliporeSigma	11796895001
DIG DNA Labeling Mix	MilliporeSigma	11277065910
Casein Blocking Buffer 10x	MilliporeSigma	B6429
CDP-*Star*®, ready-to-use	MilliporeSigma	12041677001
Qtracker 705 vascular labels	ThermoFisher Scientific	Q21061MP

REAGENT or RESOURCE	SOURCE	IDENTIFIER
TRIzol™ Reagent	ThermoFisher Scientific	15596026
SpCas9	Wolfe Lab	N/A
LbCas12a-2xNLS	Wolfe Lab	N/A
Critical commercial assays		
pGEM®-T Vector Systems	Promega	A3600
NEBuilder® HiFi DNA Assembly Cloning Kit	New England Biolabs	E5520S
mMESSAGE mMACHINE™ SP6 Transcription Kit	ThermoFisher Scientific	AM1340
MEGAscript™ T7 Transcription Kit	ThermoFisher Scientific	AM1334
Blood & Cell culture DNA Midi kit	QIAGEN	13343
NucleoSpin Gel and PCR Clean-up kit	Takara Bio	740609
MultiSite Gateway Three Fragment Vector Construction kit	ThermoFisher Scientific	12537-023
AllPrep DNA/RNA Micro Kit	QIAGEN	80284
CloneJET PCR Cloning Kit	ThermoFisher Scientific	K1231
Zero Blunt™ TOPO™ PCR Cloning Kit	ThermoFisher Scientific	451245
Experimental models: Organisms/strains		
Zebrafish: *gata2a*^{um27}	Zhu et al.[24]	ZDB-ALT-111201-1
Zebrafish: *foxc1a*^{p162}	Banerjee et al.[30]	ZDB-ALT-140721-2
Zebrafish: *Tg(ubi:CtoH2b-cherry)*^{ih63}	Zhang et al.[40]	ZDB-ALT-151007-31
Zebrafish: *gata2a*^{um345} (aka *gata2a*^{fl})	this study	um345
Zebrafish: *foxc1a*^{um383} (aka *foxc1a*^{fl})	this study	um383
Zebrafish: *rasa1a*^{um414} (aka *rasa1a*^{fl})	this study	um414
Zebrafish: *rasa1a*^{um255}	this study	um255
Zebrafish: *rasa1a*^{um290}	this study	um290
Zebrafish: *ruvbl1*^{chb10} (aka *ruvbl1*^{fl})	this study	chb10
Zebrafish: *Tg(gata2aECE:iCre)*^{um337}	this study	um337
Oligonucleotides		
See Supplementary Table 4 for all oligonucleotide sequences		
Recombinant DNA		
Plasmid: pKHR8	Hoshijima et al.[17]	RRID:Addgene_74625
Plasmid: p3E-MCS1	Moore et al.[52]	RRID:Addgene_49004
Plasmid: pmE-CreERT^2	Mosimann et al.[56]	RRID:Addgene_27321
Plasmid: pToneDest	Shin et al.[55]	RRID:Addgene_67691
Plasmid: pToneTP	Shin et al.[55]	RRID:Addgene_67692
Plasmid: p5E-6xgata2aECEbas	Shin et al.[55]	RRID:Addgene_132968
Plasmid: pCSDest2	Villefranc et al.[53]	RRID:Addgene_22424
Plasmid: pBSIce-gata2aKI	this study	N/A
Plasmid: pBSIsce-KI	this study	N/A
Plasmid: pCS-CreNS	this study	N/A

REAGENT or RESOURCE	SOURCE	IDENTIFIER
Plasmid: pCS-zfCre	this study	N/A
Plasmid: pDR274-gata2a_3pex5sgRNA1	this study	N/A
Plasmid: pJET-mCherry	this study	N/A
Plasmid: pJET-mVenus	this study	N/A
Plasmid: pKHR8-foxc1aKI	this study	N/A
Plasmid: pKHR8-rasa1aKI	this study	N/A
Plasmid: pmE-CreNS	this study	N/A
Plasmid: pmE-MCS1	this study	N/A
Plasmid: pmE-zfCre	this study	N/A
Plasmid: pmE-zfCreERT^2	this study	N/A
Plasmid: pTol1-gata2aECe:CreERT^2;cryaa:mcherry	this study	N/A
Software and algorithms		
ZEN2010	Zeiss	RRID:SCR_014340
MultiTime Series PLUS Macro	Zeiss	RRID:SCR_014340
AxioVision SE64 Rel 4.9.1 software	Zeiss	RRID:SCR_002677
Adobe Photoshop CC	Adobe	RRID:SCR_014199
Adobe Premiere CC	Adobe	RRID:SCR_021315
Adobe Illustrator CC	Adobe	RRID:SCR_010279
ImageJ2 version 2.3.0/1.53q with FIJI	NIH	RRID:SCR_002285
IC Capture 2.5 software	IMAGINGSOURCE	https://www.theimagingsource.com/enus/support/download/iccapture-2.5.1525.3931/
Prism	GraphPad Software	RRID:SCR_002798
R Package for Statistical Computing	www.r-project.org	RRID:SCR_001905
Other		
Scanning Electron microscope	Hitachi High-Technology Corp	SU8010
710NLO confocal/two-photon microscope	Zeiss	RRID:SCR_017377
Leica Fluorescence Dissection microscope	Leica	M165FC
Digital camera, AxioCam	Zeiss	MRc5
Axioskop2 Plus	Zeiss	N/A
Imaging source USB CCD B&W 2.0 camera	IMAGINGSOURCE	DMK21AU04
Spectrolinker™ UV Crosslinker	Spectronics Corp	XL-1000
hybridization incubator	Robbins Scientific	Model 400
ChemiDoc	BIO-RAD	12003153
StepOnePlus Real-Time PCR Systems	ThermoFisher Scientific	RRID:SCR_015805
Nylon Membrane, positively charged	MilliporeSigma	11209299001
Hybridization Bags	Cosmo Bio Co	SE-S-1002-EX